UNIVERSITY OF CALIFORNIA, SAN DIEGO

Universal Digital High Resolution Melt Platform for First Pass Screening of Sepsis

A thesis submitted in partial satisfaction of the requirements for the degree Master of Science

in

Bioengineering

by

Hannah Elizabeth Mack

Committee in charge:

Professor Stephanie Fraley, Chair
Professor Todd Coleman
Professor David Gough
Professor Shelley Lawrence

2017

The Thesis of Hannah Elizabeth Mack is approved and it is acceptable in quality and form for publication on microfilm and electronically:

_____

_____

_____

_____
Chair

University of California, San Diego

2017

DEDICATION

In memory of my mom, Jean Merrick-Mack. Life does not always go as planned, but I did it! I hope I continue to make you proud. Love you always.

TABLE OF CONTENTS

LIST OF ABBREVIATIONS

NICU – Neonatal Intensive Care Unit

CFU – Colony Forming Unit

GBS – Group B Streptococcus

CDC – Center of Disease Control and Prevention

VLBW – Very Low Birth Weight (<1500 grams)

ESI – Electrospray Ionization

MS – Mass Spectroscopy

FDA – U.S. Food and Drug Administration

CE – *Conformité Européenne*

PCR – Polymerase Chain Reaction

SIRS – Systematic Inflammatory Respiratory Syndrome

NPV – Negative Predictive Value

ER – Emergency Room

ICU – Intensive Care Unit

ITS – Internal Transcribed Spacer

U-dHRM – Universal Digital High Resolution Melt

HRM – High Resolution Melt

dPCR – Digital PCR

SVM – Support Vector Machine

RT-qPCR – Reverse Transcription Quantitative Polymerase Chain Reaction

AUC – Area-Under-Curve

ROC – Receiver Operating Characteristic

LAMP – Loop-Mediated Isothermal Amplification

IC 3D – Integrated Comprehensive Droplet Digital Detection

EMR – Electronic Medical Records

HRC – Heart Rate Characteristics

CCA – Canonical Correlation Analysis

SSVM – Sparse Support Vector Machine

BUN – Blood Urea Nitrogen

RR – Respiratory Rate

SBP – Systolic Blood Pressure

λ – Average Occupancy

LIST OF FIGURES

LIST OF TABLES

ACKNOWLEDGEMENTS

I would like to thank Professor Stephanie Fraley for her guidance and support as the chair of my committee.

I would also like to acknowledge all the members of the Fraley Lab, past and present. Without your continued guidance and support, in lab and in life, I would be lost.

Chapter 1, in full, is currently being prepared for submission for publication of the material. Sinha, Mridu; Jupe, Julietta; Mack, Hannah; Lawrence, Shelley; Fraley, Stephanie. The thesis author was a co-author of this material. She assisted in the Ideal Sepsis Characteristics section and the organization of the text. She also edited and formatted the whole document.

Chapter 2, in full, is currently being prepared for submission for publication of the material. Sinha, Mridu; Jupe, Julietta; Mack, Hannah; Lawrence, Shelley; Fraley, Stephanie. The thesis author was a co-author of this material. She worked on the LAMP, IC3D and U-dHRM sections. She also edited the whole document, assisted in the organization of the text and formatting, and Table 1. She also created Figures 1-3.

Chapter 3, in full, is a reprint of the material as it appears in Scientific Reports 2017. Velez Ortiz, Daniel; Mack, Hannah; Jupe, Julietta; Hawker, Sinead; Kulkarni, Ninad; Hedayatnia, Behnam; Zhang, Yang; Lawrence, Shelley; Fraley, Stephanie I. Macmillan Publishers Limited, 2017. The thesis

author was a researcher and co-author of this material. She assisted in developing the experimental procedure and conducted the experiment with the mock blood sample. She also generated Figure 8 and did the final edits of the text for submission.

VITA

2012   Bachelor of Science, Mechanical Engineering, University of
            Dayton

2017   Master of Science, Bioengineering, University of California, San
            Diego

PUBLICATIONS

"Shuttle Lock Suspension Supplemented with Suction for a Person with
Transfemoral Amputation: A Case Report" Journal of Prosthetics and Orthotics
Vol. 25, Issue 4, p 188-192, October 2013

"Massively parallel digital high resolution melt for rapid and absolutely
quantification quantitative sequence profiling" Scientific Reports 7, Article
number: 42326, February 2017

ABSTRACT OF THE THESIS

Universal Digital High Resolution Melt Platform for First Pass Screening of
Sepsis

by

Hannah Elizabeth Mack

Master of Science in Bioengineering

University of California, San Diego, 2017

Professor Stephanie Fraley, Chair

Sepsis is a life-threatening condition that results from a severe immune
response to a bloodstream infection. Identifying sepsis-causing organisms
rapidly and accurately within a clinically relevant time-frame remains a
significant challenge. To properly identify sepsis-causing pathogens, the ideal

diagnostic should be: (a) rapid, (b) broad-based, (c) capable of polymicrobial detection, (d) highly sensitive and specific, (e) minimally invasive, (f) easily integrated into clinical workflow, (g) able to detect antibiotic resistance determinants, (h) and able to identify new and unknown pathogens. The current gold standard for pathogen detection is blood culture which has limited sensitivity and detection capabilities and requires a significant amount of time. Other technologies have been developed to address some of the ideal sepsis criteria; although many meet several of the criteria for the ideal sepsis diagnostic, none have successfully fulfilled them all. We have developed a novel device that meets each of these criteria; it can identify sepsis-causing bacteria at a clinically relevant load for neonatal sepsis within four hours through an integrated system which incorporates universal PCR amplification, High Resolution Melt across a 20,000 well microfluidic chip and a machine learning algorithm. The bacterial DNA is separated by digitization across the picoliter-sized wells and the 16S gene is targeted and amplified using universal primers. This device fingerprints each well simultaneously and compares them to a library of characterized curves by utilizing a machine learning algorithm. This technology could be a valuable clinical addition as an ideal sepsis diagnostic.

CHAPTER 1: INTRODUCTION

1.1 Current status of sepsis

1.1.1 Incidence & consequence

Sepsis is a serious and life-threatening clinical condition that generally results from a primary bacterial infection or more rarely a fungal and/or viral infection. Septic patients usually present with malaise, fever, chills, and leukocytosis, which often prompts care providers to evaluate for the presence of bacteria in the bloodstream (bacteremia) using blood culture analysis. Considered a medical emergency, bacteremia can rapidly progress to organ dysfunction and death despite immediate and aggressive medical therapies[1]. Because of the high mortality rate associated with bacteremia, the dangers of undertreating some infections, or concerns about using inappropriate antibiotics, physicians tend to order blood cultures liberally[1]. However, bacteria are isolated in only 4-12% of processed blood culture tests and this occurs days to weeks after the patient has been treated[1–4].

Alarmingly, the incidence of bloodstream infections is increasing, with a rise of 17% in documented cases between 2000 to 2010[5], while sepsis-related deaths have surged 31% between 1999 and 2014[6]. In the United States, the incidence of adult bacteremia is approximately 10 per 1000 hospital admissions[7–9]. Mortality rates are associated with approximately 30,000 deaths annually with particularly high rates in critically ill patients admitted to

intensive care units[1,5,10]. Septicemia, a severe form of bacteremia, affects nearly 1 out of every 23 hospitalized patients (4.2%) and is the sixth most common reason for hospitalization[5,11]. At present, septicemia is the most expensive condition treated in U.S. hospitals with an aggregate cost of $15.4 billion in 2009, or 4.3% of all hospital expenditures[5,11], whereas non-specific diagnoses of sepsis account for another $23.7 billion each year[12,13]. Almost two-thirds of patients will contract their primary infection outside the hospital and the majority will have one or more pre-existing comorbidities[1]. Additionally, survivors of sepsis may experience substantial long-term complications including prolonged length of stay, discharge to a long-term care setting, or death[12].

Neonates, or infants within 28 days of life, comprise an additional at-risk group for infection due to the relative deficiency of their adaptive immune responses from lack of antigen exposure in utero as well as immaturity of innate immune responses; impairments which are directly related to their gestational age at birth. Worldwide, infectious disease is the second leading cause of neonatal mortality and results in the loss of one million newborns annually (half in the first week of life)[14,15]. In the United States, sepsis is the fifth leading cause of neonatal mortality, surpassed only by complications related to prematurity and pregnancy[16]. Low birth weight premature infants have a 10-fold increased risk of serious infection or sepsis compared to their full-term counterparts with a 30% mortality rate[17–19]. Devastatingly, 25% of all

neonates in the U.S. admitted to the Neonatal intensive Care Unit (NICU) will be diagnosed with sepsis and 18-35% (21,000/year) will die from their infection[14,20,21]. Pathogen detection by blood culture methods is unfortunately worse in this vulnerable patient population when compared to older children and adults. Although more than 60% of sepsis evaluations will occur in the first three days of life, less than 1% of blood culture tests will detect an organism. Even in symptomatic neonates, blood culture methodologies can detect the offending microorganism in only 10-15% after contaminants are excluded[22,23]. This burden is even more dire in underserved communities. For example, in the U.S., black preterm neonates have the highest incidence of and case fatality from neonatal sepsis[24]. Around the world, newborns born in low and middle income countries suffer the greatest rates of sepsis due to disproportionately high rates of home births in unsanitary conditions[25]. Critically, resistant bacterial strains are implicated in the majority of cases highlighting the need for rapid susceptibility testing. Survivors of neonatal sepsis are at an increased risk for poor neurodevelopmental outcomes including cerebral palsy, deafness, blindness, and cognitive delays[14,26].

1.1.2 Clinical challenges

Under-recognition of illness in addition to the emergence of resistant pathogens, delay in diagnosis, and the inability to access or afford specialized medical care contribute to the high mortality and morbidity associated with

sepsis[27]. The likelihood of surviving sepsis decreases with each hour that a patient goes undiagnosed and/or is inadequately treated[28]. Unfortunately, the current diagnostic methods used in clinics are not able to influence clinical decision making within this critical time frame. Blood cultures take 2-5 days to finalize results. Other, faster adjunct standard hematological analysis used in clinics, have low sensitivity and specificity[29]. Recently, biomarkers such as C-reactive protein, Procalcitonin, CD64 neutrophil markers have made their way into clinics with limited success due to limited sensitivity or specificity.

Clinically, sepsis presents as a complex multifactorial syndrome, yet most diagnostic approaches that are currently employed rely on individual biomarkers, with binary, yes or no, answers. There remains a significant need for a diagnostic strategy that incorporates multiple sensitive biomarkers instead of using single binary modalities. The absence of a such a robust diagnostic fosters empiric antibiotic treatment that is not evidence-based and relies instead on a clinician's best judgement. In the case of the vulnerable neonate population, clinical signs related to sepsis can be similar to other non-infectious life threatening conditions in neonates, such as perinatal asphyxia and respiratory distress syndrome. Hence, the accurate diagnosis of infectious disease is imperative to limit antibiotic exposure in non-infected neonates, while appropriately and aggressively treating those who are truly septic. The use of immediate broad spectrum and highly potent antibiotic treatment in patients suspected of having sepsis has given rise to a practice that is

implicated in the emergence of drug-resistant organisms and atypical pathogens. The correct initial choice of antibiotic therapy alone has been shown to save more lives than any other medical intervention[30–33]. For these reasons, the Surviving Sepsis Campaign advocates for diagnostic identification of a pathogen within one hour and prior to the administration of antibiotics[30]. Additionally, diagnostics that can profile antimicrobial resistance markers can assist with antibiotic stewardship, but must integrate easily into the clinical work flow. To be useful in a clinical setting, sepsis diagnostics should be easy to use and require low technical expertise to both run and interpret results.

1.2 The ideal sepsis diagnostic

Based on the current clinical challenges and to impact clinical progression towards targeted treatment, the ideal technology should include the following characteristics:

(a)   Rapid detection, the pathogen needs to be identified within 1-3 hours;

(b)   Broad-based detection, including bacteria, viruses and fungi;

(c)   Minimally invasive clinical samples with acceptable volumes. For pediatric patients, if using blood, the volume should be under 1mL (for adults, 5-10mL of blood is acceptable);

(d)   Have high sensitivity and specificity to influence empiric antibiotic use in the presence of signs for systemic inflammation. Diagnostic should not compromise on sensitivity with low levels of pathogen in the specimen;

(e)   Able to detect polymicrobial infection or pathogens in the presence of contaminants across a wide range of pathogen loads;

(f)   Incorporate detection of antibiotic resistance determinants;

(g)   Integrate into clinical work flow: Be easy to use, require low technical expertise to run diagnostics and interpret results;

(h)   Be able to identify new and unknown pathogens and continue to expand detection capabilities without compromising on the robustness of detection and required specimen volume.

1.3 Limitations of diagnostic blood culture

Robert Koch first described the use of agar culture plates for the purification and identification of disease-causing bacteria in the early 1880's, forming the foundation of modern blood culture technology[34]. Today, the use of standard culture techniques for the detection and isolation of pathogenic organisms from a sterile body fluid is considered the "Gold Standard" for the diagnosis of infection and sepsis. However, this technology is plagued by many complicating factors.

First, the quantity of microbes present in circulation during a bloodstream infection is usually low, ranging only from 1 to 1×10^4

CFU/mL[26,35–37]. Although current laboratory protocols can capture the causative organism in 73 – 96% of cases, large blood sample volumes are routinely required. Presently, blood culture tests in older children and adults are drawn in timed sequences, including up to four separate replicates that contain approximately 40 to 80 mL of blood volume each[37–39]. Pathogen detection improves with increasing numbers and volumes of blood samples analyzed. Small sample volumes can, conversely, lead to false-negative results[40–42].

False-negative results can also occur secondary to infectious etiologies not readily recovered by routine blood culture techniques and blood collection after initiation of antibiotic therapy, which affects 28-63% of adults with suspected sepsis[30,37,42–44]. Exposure to antimicrobials prior to blood culture testing is magnified in neonatal patients, as an estimated 30-35% of laboring women receive empiric intrapartum antibiotics for the prevention of neonatal *Group B Streptococcus (GBS)* disease[19]. Subsequently, compliance with the Center of Disease Control and Prevention (CDC) GBS guidelines exposes an estimated 65% of very low birth weight infants (VLBW, birth weight < 1500 grams) to antibiotics prior to birth[45–47]. Decreased total blood volume, especially in VLBW premature infants, also restricts blood collection to a single sample with minimal volume (1 mL), which can further hinder pathogen capture, particularly when bacteremia is low[48–50]. Prolonged delays in pathogen identification and antibiotic sensitivity testing, which can take up to

4-5 days, also causes neonates to be unnecessarily exposed to broad-spectrum antibiotics, leading to bacterial antibiotic resistance in non-infected neonates while preventing targeted antimicrobial therapy in septic neonates. Additionally, prolonged broad-spectrum antibiotics exposure in neonates can lead to invasive fungal (Candida) infection, necrotizing enterocolitis, and/or death[20,21,51].

Failure to adhere to standard antiseptic procedures during sample collection can also lead to contaminated, or false-positive, blood culture results. In 2005, The College of American Pathologists reported an overall mean blood culture contamination rate of 2.89% in 356 institutions, with 2.08% noted in neonatal and 2.92% for non-neonatal patients[52]. Contamination rates for individual institutions in this study ranged from 2.15% to 3.67% and contributed to an additional estimated cost of $5,506 per patient[52]. Thus, contaminated samples can have enormous financial and clinical ramifications in adult populations in the U.S. including 1,372 to 2,200 extra hospital days and an extra $1.8 to $1.9 million in medical costs each year[53,54]. In pediatric patients, these tainted samples are associated with readmission rates of 14 – 26%[42,55,56] and increased length of stay from 1 to 5.4 days[42,54,57]. In low and middle income countries, where there is a dearth of trained medical staff and quality health care services, blood culture contamination is not uncommon and can have grave consequences. Notably, almost half of patients with false-positive blood cultures are treated with antimicrobials as compared to those

with true positive test results[42,58–60]. Additionally, 40 - 50% of adult patients

with bacteremia (and 70% with fungemia) received incorrect antimicrobial

therapy during their empiric treatment period before the microbiology culture

result was available[5,7,61]. This misuse of antimicrobial agents and delays in

pathogen identification cause prolonged exposure to broad spectrum

antibiotics, which can also result in an increased number of Clostridium difficile

infections, antibiotic allergic reactions and drug toxicity, antimicrobial-resistant

bacterial strains, prolonged length of stay, and medical costs[5,42,62–64].

In summary, routinely used blood culture methods are not an ideal

"Gold Standard", as the results often come too late, are incomplete or not

sensitive enough, and can be misleading and relatively labor-intensive. There

is a crucial unmet need to shorten as well as improve current laboratory

procedures for the detection and identification of microorganisms. In the last

decade, various engineering innovations have generated promising pathogen

detection approaches that incorporate sample preparation, molecular

detection, automation, miniaturization, multiplexing, and high-throughput

analysis towards the development of an effective diagnosis technology. The

following sections give an overview of current and emerging detection systems

designed for rapid, sensitive, and cost-effective diagnosis of bloodstream

infections.

Chapter 1, in full, is currently being prepared for submission for publication of the material. Sinha, Mridu; Jupe, Julietta; Mack, Hannah; Lawrence, Shelley; Fraley, Stephanie. The thesis author was a co-author of this material. She assisted in the Ideal Sepsis Characteristics section and the organization of the text. She also edited and formatted the whole document.

CHAPTER 2: CURRENT AND EMERGING TECHNOLOGIES FOR RAPID

DIAGNOSIS OF MICROBIAL INFECTIONS WITHOUT CULTURE

Molecular diagnostics used in the United States are primarily post-culture technologies. Several diagnostic methods have been developed in the past few years that permit targeted identification of the microorganism(s) in *post-growth*, positive blood cultures within 20 minutes to 2 hours with high sensitivity and specificity. However, the time required for routine bacterial culture and growth before analysis limits their influence on antibiotic stewardship programs to de-escalate empiric antibiotic therapy and encourage timely targeted treatment. Furthermore, most are not broad-based and leave antibiotic sensitivity testing for evaluation by conventional methods. Recent reviews by Opota *et al.*[37,65], Kothari *et al.*[66], Afshari et al.[67] and Ecker *et al.*[68], describe the state of the art for such BSI diagnostic technologies in more detail. In this review, we focus on emerging technologies for identification of microbes without the need for culture. All described technologies in the following paragraphs are summarized in Table 1.

Table 1: Emerging technologies for rapid diagnosis of bacterial infections directly from blood

Assay	Technique	Sample Volume	Sensitivity	Specificity/ Accuracy	Breadth of Detection	Polymicrobial Detection	Antibiotic resistance information	Limitations
Iridica, Plex-ID platform Abbott Molecular	Multiplex broad-range PCR/ESI-MS	5 mL	83%	94%	Currently 780 bacteria and Candida Highly expandable	Yes with semi-quantification of load, limited clinical validation	four antimicrobial resistance markers (mecA, vanA/B, and blaKPC)	Use in young children/infants due to 5 ml blood required; Detection of four antibiotic resistance markers to date
LightCycler SeptiFast Test MGRADE Roche Diagnostics	Multiplex braod range or specific primer/probe PCR/insitu Hybridization/Melt Analysis	1.5 mL	43%-80%	86%-98%	25 pathogens Low expandability	Yes, limited clinical validation	mecA antibiotic resistance gene after testing positive for Staphylococcus aureus	Detection of one antibiotic resistance marker
SepsiTest™-UMD Molzyme	Universal PCR/sequencing	1 mL (capability of processing up to 10 mL)	85%-88%	83%-86%	>345 bacteria Highly expandable	Yes, limited clinical validation	no antibiotic resistance marker	No antibiotic resistance markers
Digital high resolution melt (U-dHRM)	dPCR amplification U-dHRM Machine learning	1 mL	Single-cell	99.90%	Currently 37 bacteria Can include more bacteria, viruses and fungi Highly expandable	Resolve all organisms with absolute load quantification, need clinical validation	Can be added in the future	Automation of unexpected pathogen discovery
Oxford Nanopore MinION Oxford Nanopore Technologies	Nanopore Sequencing	10 ng high molecular weight DNA (bacteria identification is not validated in whole blood)	About 100 copies per mL	97-100%	No integrated platform for broadbased detction Highly exandable	Potentilally yes with load quantification	Potential to include	Routine implementation into clinical setting; Bioinformatic pipeline is needed for analysis; Improvement of sequence quality
LAMP technology	Loop-mediated isothermal amplification	Varies on specific LAMP technique used (~30 uL to a few mL)	Single-cell	100%	No integrated platform for broadbased detction Highly exandable	Limited	Could detect 1 antibiotic resistance gene at a time in a separate sample	Limited choice of only Bst-polymerase; Optimization of loop-primers for target detection
Integrated Comprehensive Droplet Digital Detection technology (IC 3D) Velox Biosystems	DNAzyme-based sensors droplet microencapsulation 3D particle counter system	Microliters to milliliters of diluted blood	Single-cell	n/a yet	No integrated platform for broadbased detction Highly exandable	Limited	Can be added in the future; limited by number of flourescent channels available	Detection of only one type of bacteria per analysis
SeptiCyte Lab Immunexpress	RTq-PCR to quantify the host response of 4 RNA biomarkers Machine learning	2.5 mL	n/a (able to discriminate SIRS from sepsis with AUC ~ 0.9)	95%	All pathogens	n/a	No	Results need to be evaluated in conjunction with other clinical signs/symptoms or follow-up diagnostic devices

2.1 Nucleic Acid Amplification Technologies

2.1.1 Pathogen targeted PCR-based technologies

In this section, we review five Nucleic Acid Amplification Technologies (NAAT). These technologies rely on an initial multiplexed or universal amplification reaction in either a large volume or small volume digital reaction format to increase low-level pathogen DNA to a detectable amount. This is subsequently followed by identification of the microbial species represented by the DNA sequence. The second step is accomplished by using electrospray ionization (ESI) with Mass Spectroscopy (MS), in-situ probe hybridization with melt analysis, sanger sequencing, nanopore sequencing, or digital amplicon melt analysis, with varying degrees of success in achieving the goals of the ideal sepsis diagnostic.

2.1.1.1 IRIDICA BAC BSI (Abbott Molecular)

The IRIDICA platform (Abbott Molecular, Des Plaines, IL)[68] is a commercially available (in the EU) broad-based microbial identification test with whole blood[37,69]. It can identify up to 780 bacteria and *Candida*, as well as four antimicrobial resistance markers (mecA, vanA/B, and blaKPC) within six hours from a 5 mL whole blood sample[37,70,71]. This technology is not yet approved by the U.S. Food and Drug Administration (FDA) but is *Conformité Européenne* (CE) marked, meaning that it complies with the European In-Vitro Diagnostic Devices Directive[69].

IRIDICA integrates multiplexed real-time PCR with ESI/MS. The process includes cell lysis, and automated DNA extraction from a whole blood sample, PCR-amplification using multiple broad range primers, amplicon purification and ESI-MS for species identification. The PCR-amplification targets conserved regions including the16S and 23S rRNA genes for bacteria and *Candida*, respectively. The primers have been optimized with reaction mixtures to limit interference due to human DNA. Post-PCR, amplicons are selectively enriched by removing over 98% of human DNA. Species identification is then performed on the amplicons using base composition data from ESI-MS[36,72]. Limits of detection on the IRIDICA platform ranges from 0.25-128 CFU/mL for bacteria depending on the target species and 4 CFU/mL for *Candida* spp[36,72]. IRIDICA has been evaluated in a limited number of clinical studies across patients with suspected sepsis, systematic inflammatory respiratory syndrome (SIRS) and febrile neutropenia[36,71–74]. These report a sensitivity, specificity and negative predictive value (NPV) ranging from 45% to 83%, 69% to 94%, and 80% to 97%, respectively, against conventional culture methods. The contamination rates observed with IRIDICA are slightly worse than blood culture[71–73]. By excluding the contaminants and using estimated true positives rates, improved sensitivity and specificity ranging from 77% to 91% and 87% to 99%, respectively, were achieved. True positive rates were estimated by matching pathogens in PCR test replicates or by using clinical chart and culture results from other specimens [36,71]. Significant differences

have been reported in sensitivity across ICU and ER patients (p=0.005) with

higher sensitivity seen in ICU patients[71]. More clinical validation across patient

population is needed to explain the variability in specificity and sensitivity

reported by IRIDICA. We found only one study which investigated

polymicrobial specimen where IRIDICA detected four of the nine blood positive

polymicrobial infection, identifying only one of the causative organisms for

each[74].

      This broad-based semi-quantitative technology shows promise by using

whole blood (sterile or non-sterile sample) to detect a high number of

pathogens. It can detect four antibiotic resistance markers, to date, and

benefits from the ability to expand this in future. IRIDICA can detect a mixed

pathogen population, but its utility in the clinic is currently inconclusive. It is an

end-to-end diagnostic solution with structured and easy to use workflow.

Individual steps are automated, thus reducing labor load and time to six to

eight hours with only 30 minutes of hands-on time[72,74]. However, it fails to

meet the ideal turnaround time of 1-3 hours. The use of 5 mL blood is

promising for adult patients but limits feasibility for use in pediatric patients[75].

In addition, while there is no need for trained personnel dedicated to running

the system, the technology may fall short in non-centralized clinical settings

due to dependence on multiple bulky devices and high upfront costs of about

$200,000[67].

2.1.1.2 LightCycler SeptiFast Test MGRADE (Roche Diagnostics)

SeptiFast is a commercially available (in the EU), broad-based microbe identification test for whole blood[76]. It can identify 25 bacteria and fungi within six hours from a 1.5 mL whole blood sample. In addition, it can detect the mecA antibiotic resistance gene after a sample test positive for *Staphylococcus aureus*. The technology is CE-marked and commercially available in Europe but not yet FDA approved.

The SeptiFast test integrates multiplexed real-time PCR with in-situ hybridization and melt analysis. The test uses whole blood for nucleic acid extraction under a contamination-controlled workflow. This is followed by real-time PCR amplification using either universal or specific primers targeting the internal transcribed spacer (ITS) regions between the 16S and 23S for bacterial rRNA and between 18S and 5.8S regions of rRNA genes of fungi in three parallel reactions for Gram-positive and Gram-negative bacteria and fungi[77]. PCR products are detected in real-time via four detection channels using species-specific fluorescent probes. Species identified in the same detection channel are subsequently differentiated using melting temperature analysis[77,78]. It has a reported sensitivity between 3 and 100 CFU/mL, depending on the microorganism[77]. In patient populations with suspected sepsis, SIRS, and febrile neutropenia, this resolved to a 43% to 80% sensitivity range against blood culture. It has higher reported specificity ranging from 86% to 98%[78–83]. A meta-analysis of 41 studies reported a

summary sensitivity and specificity of 68% (95 % CI 63%–73%) and 86% (95% CI 84%–89%) on a total of 10,493 SeptiFast tests compared against blood culture[84]. Low sensitivity has prevented SeptiFast from identifying culture-positive organisms in 20-30% of the cases[85]. SeptiFast Identification Software provides an integrated cut-off for isolating contaminants [78]. However, a 4-fold higher sensitivity for true CoNS detection was achieved by ignoring the software cut-off[79]. SeptiFast has been reported to resolve polymicrobial infections with higher detection rates ($\chi2 = 4.50$, $P = 0.0339$) than blood culture[86–90].

SeptiFast may be considered broad-based with coverage of the 25 most relevant pathogens for sepsis with the ability to detect mixed pathogen population. The technology reports covering 90% of the most common pathogens causing blood stream infections; however, it is missing pathogens highly relevant to neonatal sepsis. The integrated cut-off offers ways to differentiate between possible contaminants and pathogens but may require further evaluation[78,79]. The technology considerably lowers the blood volume need for testing compared to conventional technologies which could be beneficial for pediatric patients[78]. However, 1.5 mL of blood is still excessive for neonates with typical samples of 1mL. SeptiFast, when used with automated DNA extraction with MagNA (Roche), shortens the complete workflow to 3.57 hours[91] and reduces labor load. This may not be a realistic estimate for decentralized systems where 4-fold higher mean sample to result

time of 15.9 hours have been reported[92]. The diagnostic may be of added

value in the management of patients with suspected sepsis who are SeptiFast

positive but blood culture negative[93,94]. However, low sensitivity deems

negative results not actionable. Other limitations include limited antibiotic

resistance information, and the inability to expand due to a limited number of

detection channels.

2.1.1.3 SepsiTest™-UMD (Molzyme)

SepsiTest is a commercially available (in the EU) broad-based

microbial identification test with whole blood. It can identify over 345 bacteria

and fungi in 8-12 hours from a 1 mL whole blood sample[95]. The technology is

CE-marked and commercially available in Europe, but not yet FDA approved.

SepsiTest integrates universal PCR with sanger sequencing. This test

uses a unique methodology to remove background human DNA to improve the

sensitivity of PCR tests by selective lysis and degradation of over 90% human

DNA[96]. After DNA is isolated, PCR is performed with a universal primer

targeting the 16S and 18S rRNA genes for bacteria and fungi, respectively.

This takes under four hours to report for bacteremia or fungemia. Purification

and sanger sequencing follows for species detection, which takes an

additional 4-6 hours. It can detect as low as 10-80 CFU/mL with some

organism bias[97,98]. SepsiTest has reported sensitivity ranging from 11% to

87% and higher specificity from 85% to 96% when compared to blood culture

in adult and pediatric patients with SIRS, sepsis, febrile neutropenia and infectious endocarditis.[99–104]. Multiple studies reported promising NPV close to 97% against blood cluture[101,104]. Similar sensitivities ranging from 37.5% to 78.6% and specificity from 86.8% to 94.4% were observed in studies adjusting for clinical context by excluding contaminants[102,103]. Additionally, as many as 45% of PCR positive test were reported as contaminents[103]. Pathogens detected in the mixed population were often identified as a contaminant. In a patient population with 12.5% polymicrobial detection rate, only one organism was identified in three of the four blood culture positive polymicrobial specimen[101].

SepsiTest is a broad-based test that requires a small amount of blood, appropriate for both adult and pediatric patients. It can, in principle, detect polymicrobial infections; however, its ability to inform clinical decision needs to be studied. SepsiTest provides the option to automate the DNA extraction (SelectNA plus, Molzyme), making it easy to integrate into clinical workflow. However, it does not provide any information on antibiotic sensitivity. In addition, it still requires multiple steps that are not integrated into one platform, increasing the risk of contamination and turnaround time. This limits its utility for informing clinical decisions regarding targeted antimicrobial therapy. The use of sanger sequencing is the main time-limiting step for SepsiTest. Hence, it may be appropriate to combine universal PCR with a faster sequencing technology along with antibiotic resistance information. Faster next generation

sequencing technologies such as MinION by Nanopore Sequencing may be an ideal candidate.

The MinION, is a portable, real-time, USB powered DNA/RNA sequencer. It was released to researchers for alpha testing as part of an early access program in 2014[105,106]. It is a generic sequencing system, that has shown the potential for use in rapid identification of pathogen directly from blood when used with the 16S Rapid Amplicon Sequencing kit[105]. For sequencing, an ionic current is passed through the nanopore by applying a voltage across its membranes; characteristic disruptions in current are triggered by DNA nucleotides as they pass through the pores[106,107]. The technology has been validated for viral pathogen identification from 140uL whole blood in under 40 minutes with 100% sensitivity and specificity[108,109]. For bacteria, so far it has only been validated in urine and feces[109,110]. Mixed population identification was validated in a study with a genomic DNA mixture of 20 bacterial strains[111,112]. By using specific primers that amplify a wide range of bacterial 16S rRNA gene, 90% of the full-length 16S rRNA could be reconstructed. However, pathogen assignment could be completed for only 8 of the pathogens from the DNA mix of bacterial strains due to low coverage. This was attributed to challenges with PCR to amplify 16S amplicons despite the use of universal primers[111]. This points to the need for optimization and validation in whole blood, a step that is already fairly optimized by PCR-based technologies. The MinION also shows promise to identify resistances of

cultivated bacteria[110,113,114] and can complement PCR tests such as
SepsiTest.

2.1.1.4 Universal digital High Resolution Melt (U-dHRM) and machine learning on pathogen DNA fingerprints for molecular diagnosis

The Universal-digital High Resolution Melt (U-dHRM) platform is a broad-based microbial identification technology with whole blood. It can currently detect 37 bacterial pathogens with single-cell sensitivity and resolve polymicrobial infections in under four hours using less than 1 mL whole blood [115,116]. This technology is in the validation phase and not yet commercially available.

U-dHRM integrates universal digital PCR (dPCR) with high resolution melt (HRM) across a microfluidic chip containing 20,000 picoliter-sized reactions to enable single cell, probe-free differentiation and quantification of multiple bacteria in a single sample[116]. The test procedure includes DNA extraction followed by universal dPCR-amplification targeting the 16S rRNA gene. Subsequently, precise heating and simultaneous imaging are performed on all reactions for HRM analysis. This generates sequence specific melt curves by unwinding DNA amplicons in the presence of a fluorescent double-stranded intercalating dye[117–120]. Each distinct DNA sequence melts uniquely, generating a loss-of-fluorescence signature as a function of temperature that is then used for species identification. A Support Vector Machine (SVM)

classifier automatically identifies the microbial species by its melt curve [Figure 1]. U-dHRM has reported a classification accuracy of 99.9% for the 37 pathogens tested with load quantification for individual pathogens[116]. The technology was validated in a mock blood sample, demonstrating its ability to identify pathogens in the presence of excessive human DNA[116] [discussed in more detail in Chapter 3].
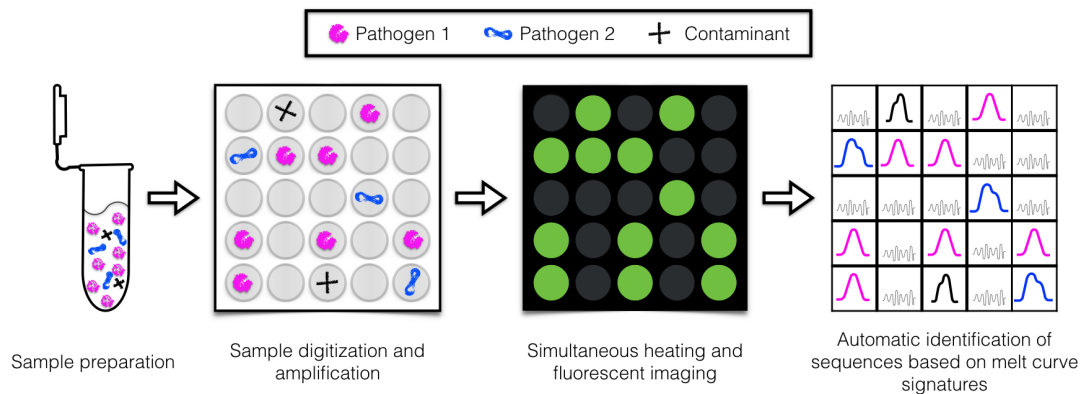
Figure 1: U-dHRM process schematic

U-dHRM is a rapid, broad-based test to detect multiple organisms in a blood sample of less than 1mL, which is suited for pediatric patients and neonates. While it is currently limited to 37 bacteria relevant to neonatal sepsis, it has the potential to expand to include additional bacteria, fungi, and viruses in the future. Since this technology is probe-free and digitized, it has the potential to detect all sepsis-causing organisms in its library from a single sample, including polymicrobial infections. Early studies show promising

single-cell sensitivity and 99.9% specificity, but further evaluation with clinical

blood samples is warranted. The system is easy to use and can incorporate

detection of antibiotic resistance determinants. Its machine learning framework

provides the potential identification of new and unknown pathogens and allows

for an expanding library. The speed and simplicity of U-dHRM along with its

integrated technology platform suggest a promising first-pass screening

method for neonatal sepsis. The technology also shows the potential to deliver

on the promise of bench-to-bedside. The ability to move towards a portable,

inexpensive system can be of immense value to non-centralized systems in

low resource settings.

2.1.1.5 Summary of Pathogen-targeted PCR-based Technologies

In summary, the results from clinical studies using PCR technologies

are heterogeneous and need to be evaluated for improving clinical outcome.

For the most part, the results are reported in comparison with the gold

standard test of blood culture, which is far from ideal. Hence, it is important to

interpret these results in conjunction with clinical context. Figure 2 compares

the processes of these technologies.
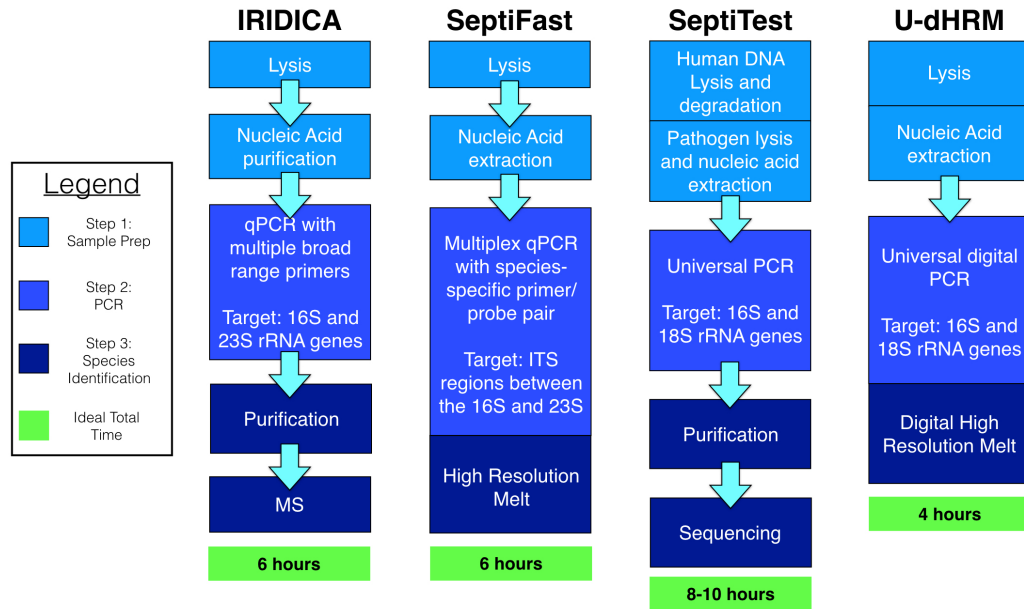
Figure 2: Comparison of the processes of the pathogen-targeted PCR-based technologies

2.1.1.5.1 Interpreting false positives against blood culture

One of the major advantages of a PCR-based technology is its ability to detect non-viable, fastidious and unculturable organisms that would otherwise be missed by blood culture. A PCR-positive, blood culture negative specimen may reflect a real pathogen, yet detecting them would lead to a biased lower sensitivity and specificity value of the PCR test. It should be noted that false positives could also be due to cell-free pathogen DNA circulating in the blood, from an old or controlled infection or contamination[121]. Both IRIDICA and SepsiTest have reported higher rates of contamination than blood culture[73,103]. First, PCR tests with broad range and universal primers are more likely to amplify and detect contaminants due to increased sensitivity. With SepsiTest,

increased handling further increases the risk of contamination[103]. SeptiFast

uses a cut-off value that represents the number of PCR cycles at which DNA

is adequately amplified to identify contaminants[79,122]. IRIDICA also uses

similar thresholds based on the number of genomes per well to limit

contaminant and reduce false positives. However, these may conversely lead

to false negatives in SeptiFast and IRIDICA and may need further

evaluation[71]. Absolute load quantification in conjugation with clinical

characteristics may allow improved identification of pathogens[122].

An emerging theme is a need for supplementing quantitative results

with clinical context, potentially provided by a machine learning framework. For

example, a diagnostic algorithm using the CD64 index as a decision maker to

perform SepsiTest showed improved detection of pathogens in patients with

suspected BSI[123]. U-dHRM overcomes these challenges by managing

contamination through the use of small reaction volumes and absolute

quantification without affecting the detection sensitivity[115]. It also integrates the

dPCR and HRM steps on a single closed system. This eliminates a sample

transfer and reduces hands-on time and risk for contamination with several

other technologies[115]. Importantly, this technology could enable further

assessment of the appearance and removal of bacterial DNA during BSI and

antibiotic treatment which could lend deeper insights into the progression of

sepsis. Having the ability to repeat tests over time to study disease dynamic

may also help in understanding pathogen detection inconsistencies that often

arise in technology comparison studies. Moreover, the effect of adequate antibiotic treatment could be monitored with decreasing relative bacterial DNA load over successive tests. U-dHRM holds promise to address this challenge as it is geared towards a point-of-care diagnostic, whereas commercially available PCR tests typically need bulky equipment and are not suited for decentralized systems.

2.1.1.5.2 Interpreting false negatives against blood culture

While false positives may result in the inaccurate overuse of antibiotics and contribute to the generation of resistant organisms, false negatives and the inaccurate withholding of antibiotic treatment are more immediately threatening to patient welfare[124]. Accurately withholding empiric antibiotic use will require an improved sensitivity of PCR technologies (>98% negative predictive value)[125]. PCR tests can be limited in their ability to detect pathogens for a variety of reasons, including the need for effective lysis across a broad range of microbes, the interference of human DNA or other inhibitory substances carried over from blood into the PCR reactions, the effect of off-target interactions, and amplification bias[126–128]. It is interesting to note that even though all the above technologies rely on an initial PCR amplification step for microbe detection followed by a secondary step for species, they differ in their diagnostic sensitives. All the commercially available PCR tests have optimized their workflow to improve pathogen amplification using DNA, yet

none show promise to replace blood culture due to limited sensitivity in clinics. Blood volumes, and blood draw sites can also impact sensitivity. The IRIDICA platform has recently increased sample volumes 5-fold, from 1 mL to 5 mL, under the assumption of uneven distribution of the pathogen[36]. The enhanced sensitivity of U-dHRM is attributed to the diluting effect of the digital reaction format on inhibitory substances and the optimized dPCR reaction conditions ensuring amplification of single copies of DNA. U-dHRM has been shown to significantly reduce false negative error rates compared to traditional dPCR, indicating that amplification errors can be reliably identified and accounted for[115]. In addition, U-dRHM is the only test that provides absolute load quantification, to enable resolution of polymicrobial infections and contamination. Still, further investigation in clinical samples is needed.

2.1.2 Host-targeted PCR-based technologies

2.1.2.1 SeptiCyte LAB (Immunexpress Inc, Seattle, Washington)

SeptiCyte LAB is the first RNA-based technology which uses specific markers from 2.5 mL whole blood to quantify host response for same-day detection of sepsis in under 4-6 hours[129]. It has 510(k) clearance from U.S. Food and Drug Administration (FDA) for use as an aid in differentiating infection-positive (sepsis) from infection-negative (SIRS) systemic inflammation in critically ill patients on their first day of ICU admission.

SeptiCyte LAB is a host response, RT-qPCR-based test that quantifies the relative expression levels of four RNA biomarkers (CEACAM4, LAMP1, PLA2G7, and PLAC8) known to be involved in innate immunity and host response to infection. In the discovery phase, microarray analysis was used to identify the relevant RNA biomarkers in a cohort of patients with sepsis and post-surgical infection-negative systemic inflammation[130]. The output of the Septicyte LAB classifier was then converted from a microarray to a reverse transcription quantitative polymerase chain reaction (RT-qPCR) format[130]. SeptiCyte Lab has been shown to be rapid, robust and accurate for the tested classifier across gender, race, age and date of ICU admission[130]. It is suggested to be an indicator of the probability and not the severity of sepsis[131,132]. In a pilot study using 2.5 mL of blood, SeptiCyte LAB test effectively discriminated between two groups of critically ill pediatric patients (40 children with clinical severe sepsis syndrome versus 30 children with congenital heart disease). Area-under-curve (AUC) in receiver operating characteristic (ROC) curve analysis was used to discriminate between the two cohorts using RNA transcript data generated by both next-generation sequencing and RT-qPCR (Applied Biosystems 7500 Fast Dx Real-Time PCR system, Thermo Fisher Scientific). In both cases, AUC value > 0.9 was obtained (0.99 vs 0.95). In another prospective observational study with 129 adult ICU patients, AUC of 0.88 was obtained to discriminate SIRS from sepsis. SeptiCyte Lab scores have shown the ability to classify sepsis better

than individual or a combination of other clinical, demographic, and laboratory markers [133].

SeptiCyte is a promising, novel, broad-based diagnostic for sepsis. The current 4-6 hours of turnaround time can potentially be reduced to a targeted 1.5 hours by optimizing the RT-qPCR platform on which the test is implemented. One drawback is the requirement of 2.5 mL of blood, which is not feasible for children and neonates. In addition, it does not provide any information about the pathogen or antibiotic resistance. Nonetheless, it can reduce inappropriate empirical antibiotic use and can add tremendous value considering the recent antibiotic resistance epidemic. More clinical studies across patient population are needed to confirm its ability to improve outcomes in the clinic. It would be synergistic to see Septicyte combined with a promising PCR test for pathogen identification and antimicrobial resistance. Sepicyte has the potential to not only provide diagnostics information, but also basic information about the progression of infection in individuals or populations of patients.

2.1.3 Loop-mediated Isothermal Amplification (LAMP)

LAMP techniques have been used extensively in the development of rapid and sensitive diagnostic assays for detection of individual bacterial species and show potential for use in molecular point-of-care diagnostics. A typical LOOP reaction can be completed in under 60 minutes[132,133] and can

amplify from a sample volume as small as a finger prick (~30 μL) up to the milliliter range of blood[136]. Compared to conventional PCR methodologies, which require thermocycling, LAMP eliminates this step through isothermal (typically 60-66 °C) amplification of nucleic acids, which potentially reduces energy costs and could enable greater access of use[137]. LAMP has the ability to amplify target nucleic acid sequences from samples that often contain substances that can inhibit PCR reactions, such as blood components of hemoglobin[137].

This method is based on autocycling strand-displacement DNA synthesis performed by the large fragment of *Bst* DNA polymerase. Typically, four different primers are used to identify six distinct regions of the target DNA. The inner set of primers initiates target amplification, while a second, outer set of primers, begin a round of strand-displacement DNA replication, regenerating a single-stranded template without the need for heat denaturation[138]. An additional pair of loop primers can further accelerate the reaction[134,135]. The use of multiple recognition sites greatly increases specificity in comparison to traditional PCR techniques. There are about nine research-based products on the market which use LAMP techniques for detecting pathogens, such as bacteria and viruses[137]. With some LAMP kits, amplicon products can be detected by the naked eye by the use of fluorescence or turbidity[138]. However, none of these are approved for clinical use. In a study of methicillin-resistant *Staphylococcus aureus*, a LAMP-based

technique demonstrated a sensitivity of 92.3%, 100% specificity, and NPV of 96.9% when applied to positive blood culture samples[139].

LAMP has been shown to be very fast, easy to use, and highly sensitive. LAMP-based microchip strategies have great potential for functional, portable devices that may be particularly useful for infectious disease diagnosis in low and middle-income countries[140]. It can potentially amplify medium-to-long-range template strands of nucleic acids and has a very high specificity due to the use of four or six different primers that bind to specific sites on the template strand. However, this approach is very specific, targeting only a single bacterial species; expanding the breath of detection may decrease its sensitivity significantly. While this technology can detect a wide range of pathogens separately, it cannot detect all the sepsis-causing pathogens at once; multiple samples would need to be run for broad-based detection, which would require a larger sample volume. Some studies suggest the use of as little as a 30 μL blood volume for detection[136]. Most sepsis cases in children are considered low-level bacteremia ($\leq$10 CFU/mL)[75]. Detection from a 30 μL volume of blood does not seem viable and may lead to false-negative results. None of the LAMP-based techniques developed for pathogen detection thus far have demonstrated the ability to detect antibiotic resistance or to identify new or unknown pathogens.

2.2 Amplification-Free Technology

2.2.1 Droplet digital detection technology

A new platform technology termed "Integrated Comprehensive Droplet Digital Detection" (IC 3D) that can selectively detect individual bacterial species directly from small quantities of whole blood within 1-4 hours[141]. In a one-step, culture- and amplification-free process, the IC 3D method provides quantitative bacterial detection at single-cell sensitivity.

IC 3D combines DNAzyme-based sensors with real-time droplet microencapsulation and particle counter. It converts blood samples directly into billions of micrometer-sized droplets containing bacteria and fluorescent DNA sensor solution. The solution contains a DNA probe conjugated to a fluorescent reporter that is cleaved upon hybridizing with a target sequence. The droplets with bacterial markers can be identified by fluorescence. A three-dimensional particle counter is then used to rapidly, robustly, and accurately quantify the fluorescent bacteria[142,143]. Distribution of the blood sample into many small droplets minimizes the interference of other components of blood, making it possible to directly detect target bacteria without purification[144]. In a study with blood infused with bacteria, the IC 3D identified *E. coli* and confirmed the presence or absence of target bacteria within an hour, whereas about 3.5 hours are typically needed to provide quantitative measurements about the number of bacteria in the samples. The assay detected bacterium about 77% of the time from samples containing 1 cell per mL[141].

This technology shows promise by its ability to detect pathogens rapidly with a small blood volume at single-cell sensitivity. Also, it is relatively easy to use and antibiotic resistance could be possible in the future by introducing additional fluorescent markers. However, the current system design is limited by its ability to detect only one bacteria species (e.g. *E. coli*) per analysis, but it has the potential to expand the sensor set and develop a multiple-wavelength detection system for multiple bacteria or pathogen detection[141]. It should be noted that the extent of this expansion would be limited by the number of fluorescent channels and could not include previously uncharacterized pathogens. The specificity has not yet been determined; this technique has yet to be validated using clinical samples.

2.3 Machine learning applied to molecular detection patterns and clinical data for diagnosis

The predictive power of machine learning techniques applied to the clinical data gathered for patients can be a valuable tool to improve diagnosis and management of sepsis. Even though it is difficult to discuss purely electronic medical record (EMR) based machine learning algorithms in light of the characteristics for ideal sepsis diagnostics, we think it is worth summarizing some of the promising machine learning approaches that have been evaluated in a clinical cohort. The addition of EMR machine learning

approaches could provide valuable information to impact clinical progression when used with any of the above diagnostics.

2.3.1 HeRO score (MPSC)

Recently, heart rate characteristics (HRC) have been used in clinics as a commercially available system, known as the HeRO score[145]. The technology uses machine learning to identify subtle irregularities in heart rate variability to provide an "early warning" of patient distress. The HRC index used by HeRO was shown to reduce mortality from 10% to 8% in a randomized controlled clinical trial of 3,003 very low birth weight infants[146]. However, this study was industry sponsored and the mechanism for mortality reduction remains unclear. An independent, academic study of HRC monitoring in VLBW infants reported a higher utilization of antibiotics and more sepsis evaluations in the cohort with HRC monitoring as compared to controls without monitoring. This study also demonstrated no differences in the rates of blood culture positive sepsis or clinically suspected sepsis, stating that the effectiveness of this technology was "no better than a coin flip"[147]. An additional single-center retrospective study reported that elevated HRC scores had limited ability to detect bloodstream infection among neonates in the NICU, emphasizing that HRC alone may not be adequate[148].

2.3.2 Other machine learning approaches for sepsis diagnostics

Unlike the HeRO score, which uses a single modality, heart rate variability, a machine learning framework also allows the incorporation of multiple diagnostic markers from large clinical datasets. One study reported the use of canonical correlation analysis (CCA) and sparse support vector machine (SSVM) classifiers to select the best subset biomarkers, such as band neutrophils, platelets, neutrophil CD64, white blood cells, and segmented neutrophils on a dataset of 1,383 sepsis evaluations from 749 neonates with suspected sepsis in the NICU[149]. Another research group developed predictive models for late-onset neonatal sepsis using EMR data from 1,826 NICU infants with 299 sepsis evaluations[150]. They developed a variety of machine learning algorithms and their models matched the treatment sensitivity and specificity of clinicians. These algorithms need to be validated in a prospective study, but present a promising opportunity for improving early diagnosis and antibiotic management practices in the NICU.

The recently developed targeted real-time early warning score is a targeted real-time early warning score that predicts which patients will develop septic shock[151]. The score incorporates a variety of physiological inputs, including platelets, ratio of blood urea nitrogen (BUN) to creatinine, arterial pH, temperature, bicarbonate, respiratory rate (RR), white blood cell count, systolic blood pressure (SBP), heart rate, and heart rate/SBP (shock index). These machine learning techniques allow the use of heterogeneous datasets to

inform clinical decisions. However, none included broad-based diagnostics.

Additionally, the use of a Bayesian framework further allows incorporation of

EMR data along with broad-based detection technologies, increasing the

reliability of the diagnostics. In the era of large-scale data integration in

electronic health records, combining broad-based techniques with EMR

presents tremendous opportunities for timely and accurate diagnosis and

management of sepsis.

2.4 Summary of emerging molecular diagnostic technologies

An exciting new era of molecular diagnostics for bloodstream infections

is emerging through innovations in sequencing, sample

partitioning/preparation, and other single-molecule detection methods, which

have the potential to identify microorganisms and provide relevant subspecies

information in a shorter time compared to blood culture [Figure 3]. Integration

of these technologies with each other and machine learning approaches

incorporating EMR data is a promising new frontier. Current commercially

available PCR technologies may not be able to replace blood culture but they

offer added advantages when used with other clinical markers for infection to

facilitate targeted antibiotic use. U-dHRM shows promise by addressing the

challenges with requirements of blood volume, higher sensitivity and the ability

to resolve polymicrobial infections in a platform that can be portable.

Innovation in the scalability of emerging technology areas of LAMP and IC 3D

could be valuable if they are able to scale to a broad-based platform without increasing the requirement for specimen volume. They may be of value in target identification for outbreaks in public health settings. With the requirement of little blood volume, LAMP could be more useful in conjunction with another device for a fast approach to detecting antibiotic resistance. FDA approval of SeptiCyte provides the clinicians a robust way to detect host response to a pathogen. A definitive yes/no on pathogen by SeptiCyte or via universal PCR tests such as SepsiTest or U-dHRM for fungi, viruses and bacteria can potentially improve clinical outcome. In the era of big data, advances in the field of machine learning can provide additional context to increase the sensitivity of any of the above-mentioned molecular diagnostics. The translation of these results from the lab to the end user or clinician in an easy and cost effective way would have to be effectively evaluated, but in general, clinical microbiology will help for the future goals to provide an effective sepsis diagnosis directly from clinical samples.
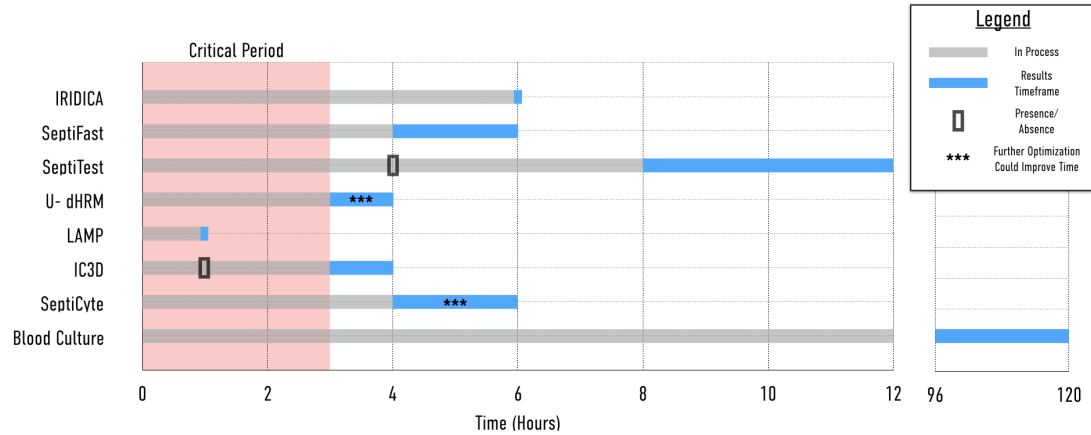
Figure 3: Sepsis detection technologies time-to-results compared to blood culture

Chapter 2, in full, is currently being prepared for submission for publication of the material. Sinha, Mridu; Jupe, Julietta; Mack, Hannah; Lawrence, Shelley; Fraley, Stephanie. The thesis author was a co-author of this material. She worked on the LAMP, IC3D and U-dHRM sections. She also edited the whole document, assisted in the organization of the text and formatting, and Table 1. She also created Figures 1-3.

CHAPTER 3: MASSIVELY PARALLEL DIGITAL HIGH RESOLUTION MELT FOR RAPID AND ABSOLUTELY QUANTITATIVE SEQUENCE PROFILING

3.1 Introduction

The rapid and accurate profiling of pathogen genotypes in complex samples remains a challenge for existing molecular detection technologies. Currently, the identification of bacterial infections relies primarily on culture-based detection and phenotypic identification processes that require several days to weeks to complete. The practical application of molecular profiling technology is limited by several factors. To replace culture, molecular approaches must capture an equally wide array of pathogens while also providing specific and sensitive identification in a turnaround time fast enough to impact clinical decision making[152–154]. Studies also suggest that quantification of pathogen load may offer added benefits beyond what culture can offer[155]. However, the number of microbial genomes present in a clinical sample may be extremely low and/or the sample may be comprised of several different microbes. Current bacteria-targeted rapid screening technologies suffer from non-specific hybridization (e.g. microarrays, FISH), non-specific protein signals (e.g. protein mass spectrometry), or limited resolution of species (e.g. nucleotide mass spectrometry)[156–158]. Sequencing with conserved primers targeting the 16S or rpoB genes is the most useful molecular approach for detecting a wide range of bacteria with broad

sensitivity, but is a time-consuming process that requires non-trivial technical expertise, computational resources, and analysis time. Moreover, recent studies report that several NGS platforms for microbial detection approach the analytical sensitivity of standard qPCR assays[154]. For applications where turnaround time is critical, high-level multiplexing of PCR-based identification strategies remain an active area of research.

High resolution melt (HRM) has gained popularity as a rapid, inexpensive, closed-tube DNA sequence characterization technique. Precisely heating and unwinding post-PCR DNA amplicons in the presence of a fluorescent intercalating dye[119,120,159] or sloppy molecular probes[160,161] loss-of-fluorescence melt curves are generated, providing unique DNA sequence signatures. Several researchers have proposed the expansion of HRM into a broad-based profiling technology by preceding it with universal PCR[162]. Priming conserved DNA regions flanking genetic variation sites or mutations, genetic locus sequence differences can be identified by changes in the gene amplicon melt curve signature. This universal HRM technique replaces the need for targeted primers or probes and relies only on the intrinsic melting properties of the amplified sequence. Universal HRM methods have been developed for several applications, including identification of oncogenic mutations[163], gene methylation patterns[164,165], and bacterial identification[166–171]. We previously advanced universal HRM to enable single nucleotide specificity for the discrimination of microRNA in the Lethal-7 family and for

species-level identification of bacteria using the 16S gene[172,173]. However, if multiple sequence variants are present, as often occurs in clinical samples, individual sequences cannot be identified in the conventional universal HRM format consisting of a single bulk reaction[162,174]. Likewise, although generally reproducible melt curves are obtained, in-run template standards are typically required to overcome run-to-run variability and enable curve matching by user intensive curve identification procedures. These shortcomings have restricted the application of universal HRM to primarily pure homogeneous samples, constrained the breadth of profiling to only a few sequence variants, and limited the technique's specificity, since single nucleotide changes often manifest as very slight temperature or curve shape changes.

We previously developed an approach called universal digital high resolution melt (U-dHRM) by integrating universal amplification strategies and temperature calibrated HRM with limiting dilution digital PCR (dPCR) in a 96-well plate format[172]. We demonstrated that this approach, in principle, could overcome many limitations of current profiling technologies to achieve single nucleotide specificity, broad-based detection, single molecule sensitivity, and absolute quantification simultaneously. Separately, we've developed machine learning approaches using nested, linear kernel, One Versus One Support Vector Machines (OVO SVM) to automatically identify sequences by their melt curve signatures despite inherent experimental variability[173,175]. Through these approaches, we've shown that U-dHRM is capable of automatically identifying

multiple distinct genotypes in a mixture with single molecule sensitivity and single nucleotide specificity. Others have also demonstrated the ability of U-dHRM to sensitively detect rare mutants/variants[176,177] and also novel variants[178]. These findings suggest that U-dHRM has the potential to offer desirable features for several profiling applications that require a combination of speed, sensitivity, quantitative power, and broad profiling ability. However, no platform exists for accomplishing U-dHRM in a high-content format required to reach a clinically relevant dynamic range of detection.

The sensitivity and quantification power of U-dHRM profiling relies on full digitization of the sample, i.e. spreading the sequence mixture across many reactions so each target molecule is isolated from others. Since the process of loading DNA into wells is stochastic at limiting dilutions, the dynamic range of single molecule detection follows a Poisson distribution, requiring the total number of reactions to be approximately 10 to 100 times the number of sequence molecules. That is, the average occupancy (λ) across all reactions must be 0.1 to 0.01 copies of DNA per well. The probability of DNA occupancy in any well, i.e. the fraction of wells having 1, 2, 3, etc. copies, is given by the Poisson probability distribution $P = (e^{-\lambda} * \lambda^{n})/n!$, where n is the total number of wells. U-dHRM is currently performed in traditional PCR multi-well plates using HRM enabled qPCR machines. In this format, only about 9 molecules in a sample can be profiled at the single molecule level per 96-well plate (Fig. 4A, left). Therefore, a major challenge to the advancement of HRM-

based profiling is the need for an exponential increase in the number of reactions to achieve scalability for realistic sample concentrations. To this end, a microfluidic U-dHRM system could offer the necessary scalability. Although several reports have documented the use of microfluidic chambers or droplets for dPCR, these platforms cannot accomplish U-dHRM. Microvalve-based dPCR devices (e.g. Fluidigm's qdPCR) do not have high resolution heating blocks necessary for high resolution melt curve generation and moreover are not programmed to capture fluorescence during heat ramping or identify sequence-specific curve signatures. Microfluidic droplet-based digital PCR devices (e.g. Bio-Rad's ddPCR) perform endpoint PCR detection in a continuous flow format without temperature control, one droplet at a time, which prevents in-situ, real-time monitoring of fluorescence in droplets, as is needed by U-dHRM. To address these challenges, we developed a platform that accomplishes massively parallelized microfluidic U-dHRM and integrated this platform with our machine learning curve identification algorithm. Our technology achieves single molecule sensitive detection and absolute quantification of thousands of bacterial DNA molecules in polymicrobial samples in less than four hours. We show proof of principle in mock blood samples that highly sensitive, specific, and quantitative bacterial identification is achieved in samples containing a high background of human DNA.
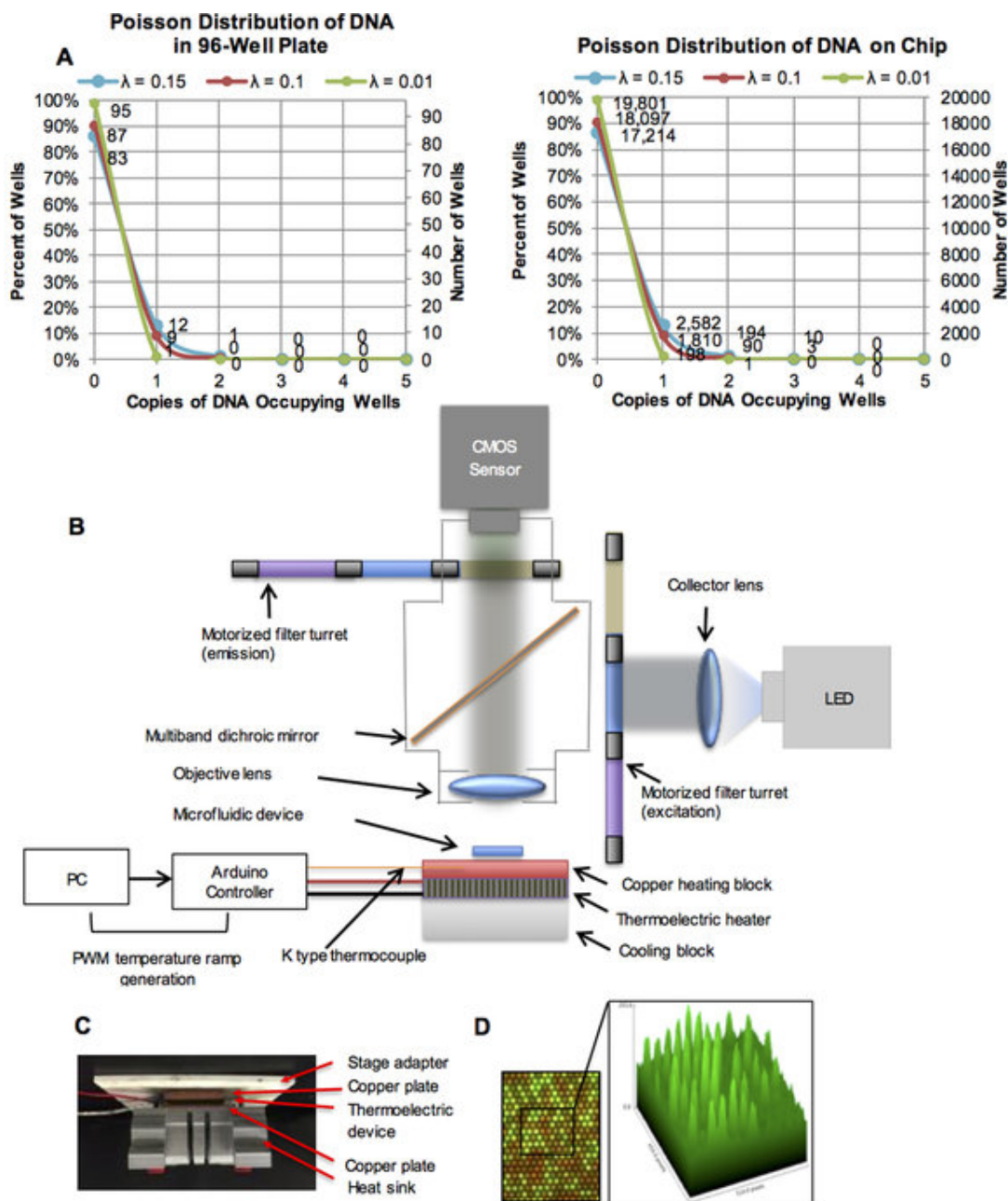
Figure 4: Massively parallel U-dHRM device.
(A) Poisson distribution of DNA in a 96-well plate versus a 20,000 well digital PCR chip, showing the distribution of molecules per well. **(B)** Schematic of the U-dHRM platform. **(C)** Image of the actual U-dHRM heating setup. **(D)** Fluorescent image of a small portion of chip where background dye (red) and intercalating dye (green) are overlaid. 3D intensity plot of the green channel is shown in inset.

3.2 Results

3.2.1 Digital HRM Device Concept

We developed our proof-of-concept U-dHRM platform for the clinical

application of neonatal bacteremia diagnosis. Clinically relevant bacterial loads

are estimated from culture techniques to be between 1 to ~2,000 colony

forming units (CFU) per blood sample (1 mL), where 76% of samples

have $\leq$50 CFU[179,180]. This load requires 20,000 reactions to provide a dynamic

range of detection up to 1,810 bacterial genomic DNA molecules at the single

molecule level (Fig. 4A, right). A digitizing chip fitting this scale of reactions is

commercially produced for traditional endpoint dPCR applications (see

Methods), and was chosen as a robust and reliable digitizing device. To

identify digitized bacterial DNA, universal primers targeting the 16S rRNA

gene were used. The 16S harbors conserved sequence regions flanking

hypervariable regions that are unique to different genus and species of

bacteria[181]. Primers targeting conserved regions generate bacteria-specific

amplicons for U-dHRM profiling. Specifically, our long amplicon (~1,000 bp)

16S bulk universal HRM assay[173] was adapted (see Methods) to enable

successful digital amplification and reliable U-dHRM in each of the 725

picoliter volume reactions on-chip, a 99.995% volume reduction compared to

the typical HRM reaction format. To enable massively parallel U-dHRM across

the 20,000 reactions, we developed a custom high resolution heating device

and imaging system. A schematic of our design is shown in Fig. 4B. Precise

chip heating was accomplished using a thermoelectric heater/cooler with Arduino controller, power supply, and heat sink. A copper plate was attached between the thermoelectric device and the dPCR chip and between the heat sink and the thermoelectric device to evenly distribute heat. A custom adapter was designed to secure the chip-heating setup onto an automated x,y stage for rapid imaging of the 20,000 reactions as four tiled images at each temperature point during the U-dHRM heat ramp. Figure 4C shows an image of the integrated heating device and stage adapter. The imaging system was equipped with a 4x objective as well as red and green LED-based fluorescence channels. An image analysis program was developed to align reaction well centroids and overcome image drift during heat ramping as well as extract raw fluorescence data from each reaction simultaneously (Fig. 4D). Our previously developed OVO SVM algorithm was adapted to classify and quantify U-dHRM curves after being trained on melt curves generated on-chip. The digital chip, chip heating device, fluorescent imaging system, control electronics, and analysis algorithms for image processing and melt curve identification were integrated to enable massively parallel U-dHRM and absolutely quantitative bacterial profiling.

Figure 5: On-chip U-dHRM process characterization and optimization.
(A) Image of a portion of a chip, which has been saturated with synthetic DNA such that nearly all wells exhibit green fluorescence of intercalating dye. Upon controlled heating, fluorescence is lost as DNA denatures. **(B)** Melting of three synthetic temperature calibrator sequences (pre-made and applied in high concentration to the chip, not PCR amplified) containing different GC content. Optimized ramp rate on-chip compared to bulk qPCR HRM. The mean and standard deviation of the calibration sequence melt curves are shown. **(C)** A plot of the relationship between voltage and temperature for 5 runs, showing it remains linear throughout the HRM temperature range of interest. Standard deviation reaches a maximum of 1.22 °C at 91.6 °C.

3.2.2 System Characterization and Optimization

The challenge of generating high quality U-dHRM curves in picoliter-scale reactions was first approached by tuning fluorescent intercalating dye concentrations to maximize signal-to-noise ratio. An EvaGreen dye concentration of 2.5X was found to be the highest concentration that did not inhibit amplification on-chip. Next, the simultaneous imaging and heating process of melt curve generation (Fig. 5A) was tuned using three synthetic DNA sequences containing 0% GC, 12% GC, and 76% GC with different predicted melting temperatures (Tms) (Fig. 5B). The greater the GC content, the higher the temperature required to melt the DNA due to higher bond strength. After loading mixtures of these three sequences onto a chip, we performed preliminary calibrations of our device, optimizing imaging exposure time to minimize photobleaching while maintaining the highest possible signal-to-noise ratio. We also used these initial readings to develop our image analysis algorithm (see Methods). Figure 5B shows the normalized fluorescence versus temperature and derivative melt plots for the three calibrator sequences in traditional qPCR HRM and U-dHRM formats. The temperature calibrators are predicted to melt at 57.3 °C, 62.8 °C, and 92.9 °C by melt curve prediction software, uMELT[120]. The average Tms given by qPCR HRM were 56.9 °C, 67.4 °C, and 90.5 °C, respectively, while U-dHRM Tms were 55.5 °C, 64.6 °C, and 83.4 °C. These readings indicated that further temperature ramp optimization was necessary. Improved temperature

resolution was achieved by varying the heating ramp rate until a linear and repeatable relationship between voltage and temperature could be maintained throughout our temperature range of interest, 45–95 °C. For highest accuracy, temperature was monitored during the ramp by placing a thermocouple inside a surrogate oil-filled chip and placing this chip next to the calibrator loaded chip. A ramp rate of 0.02 °C/sec was found to give optimal linearity and repeatability of the voltage and temperature relationship, with maximum standard deviation of 1.22 °C occurring at a temperature of ~91.6 °C over 5 runs (Fig. 5C).

Next, bacterial DNA from clinical isolates of *Listeria monocytogenes* and *Streptococcus pneumoniae*, two common pathogens causing neonatal bacteremia[182], were used to further optimize signal-to-noise ratio and melt curve shape resolution (i.e. temperature resolution). First, HRM optimization was carried out on a standard qPCR HRM machine. In this format, melt curve shape, a key discriminating feature of bacterial 16S melt curves[173], was found to be highly dependent on imaging rate. A low imaging rate of 1 image per 0.3 °C smoothed melt curve shape features (Fig. 6A, circle), but a faster imaging rate of 1 image per 0.1 °C captured small shape differences known to be identifiable by our machine learning algorithm[173] (Fig. 6C, circle). Using the optimized chip heating ramp rate described above, we next optimized imaging rate on the standard qPCR HRM machine and validated these settings on our U-dHRM system (Fig. 6B and D). The low

calibrator sequence (first peak from left in Fig. 6 melt curves) was included in all amplification reactions to align curves and overcome temperature variation across reaction wells. First, the chip imaging rate was adjusted to replicate the default qPCR machine of 1 image taken every 0.3 °C. Imaging the chip every 15 seconds at the optimal heat ramping rate of 0.02 °C/sec on our U-dHRM platform allowed us to achieve this rate. Melt curves generated from these settings constitute the low imaging rate data in Fig. 6B. With these settings, the average peak-to-baseline ratio of the 16S amplicon derivative melt curves (after min-max normalization of raw melt data) was 0.1096±0.0024 on the qPCR HRM machine versus 0.0660±0.0034 for U-dHRM. We then increased the imaging rate on our U-dHRM system to image every 5 seconds, matching the high imaging rate of 1 image per 0.1 °C on the qPCR HRM machine (Fig. 6D). At the high imaging rate, the average peak-to-baseline ratio of the 16S amplicon derivative melt curves was 0.1759±0.0073 on the qPCR machine versus 0.1225±0.0066 for U-dHRM, demonstrating that our device achieves comparable signal-to-noise performance. Small shape differences in melt curves were also identifiable on-chip but to a lesser degree than in the standard qPCR HRM machine (Fig. 6A–D, circles). However, higher background noise on-chip caused this detail to occasionally be lost during curve processing and normalization (Fig. 7A, bottom). Tm reproducibility was almost identical between the two optimized platforms, as demonstrated by the Tm standard deviation of the temperature calibrator sequence (~0.3 °C, Fig.6).

Because this deviation still existed under optimized conditions, temperature calibrator sequences were included in all reactions for aligning melt curves prior to further analysis.

We then integrated our automated OVO SVM melt curve identification approach with our U-dHRM platform to enable automated identification of bacteria based on their melt curve signatures. A training database of bacterial melt curves was generated on-chip to enable automatic curve identification. Bacterial DNA from *L. monocytogenes* and *S. pneumoniae* were loaded onto separate chips in excess, λ of 223 and 141, respectively, as calculated from spectrometer readings. This ensured each of the 20,000 reactions would be positive for amplification and would generate a training melt curve for the bacterial isolate. Each sample underwent U-dHRM using the optimized ramp and imaging rates described above. Figure 7A shows the U-dHRM training curves generated on-chip for *S. pneumoniae* and *L. monocytogenes* after processing with our image analysis, normalization, and alignment algorithms (see Methods). The processed curves were entered into our OVO SVM algorithm as training data (see Methods). Leave One Out Cross Validation (LOOCV) reached a maximum classification accuracy of 99.9% within the training dataset with 1,500 training curves.
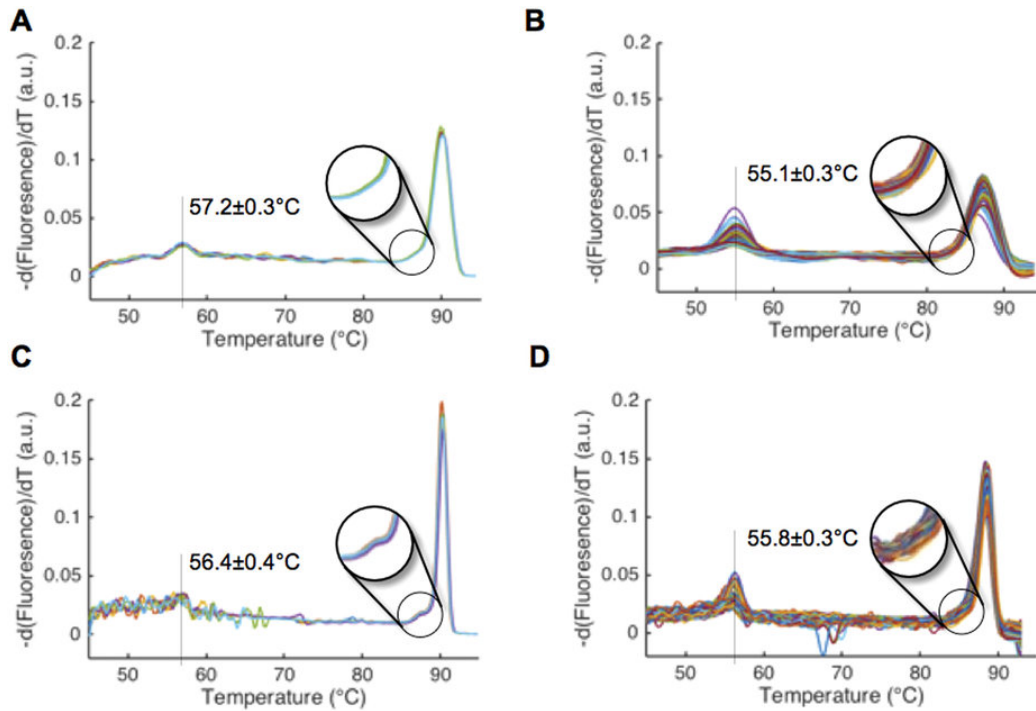
Figure 6: U-dHRM sampling and ramp rate optimization on chip.
(A,B) *L. monocytogenes* melt curves generated with a low imaging rate on qPCR HRM and U-dHRM platforms respectively. **(C,D)** *L. monocytogenes* melt curves generated using a high imaging rate on qPCR HRM and U-dHRM platforms respectively. The synthetic temperature calibrator sequence mean melting temperature and standard deviation are shown in all. Black circle highlights a melt curve shape feature unique to *L. monocytogenes* 16S sequence, which is dependent on sampling rate.
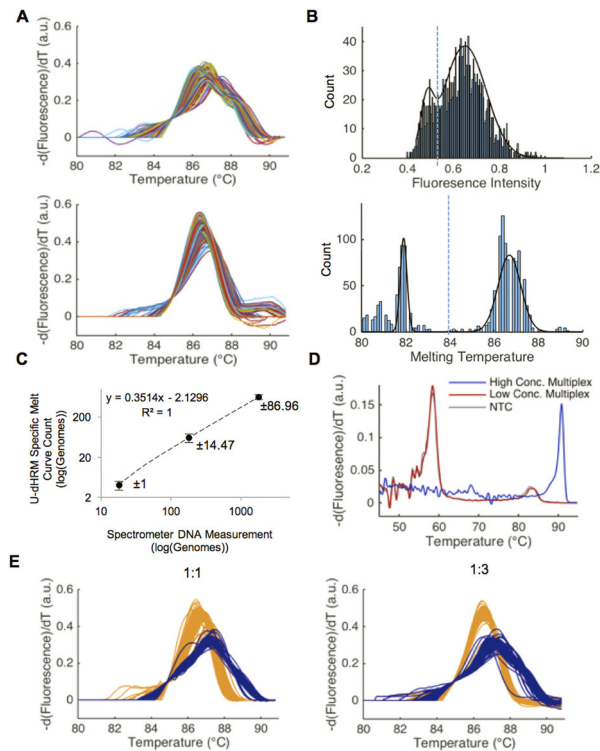
Figure 7: OVO SVM classification of *L. monocytogenes* and *S. pneumoniae*.

(A) Two-thousand normalized *S. pneumoniae* **(top)** and *L. monocytogenes* **(bottom)** U-dHRM melt curves aligned to 0.1 –dF/dT, respectively. These curves were used to train the OVO SVM to classify each bacteria. **(B)** Histogram of fluorescence intensity values of digital reaction wells with PDF overlay and the intensity value chosen to classify positive from negative marked by dotted line (top). Histogram showing the Tm of each digital reaction with PDF overlay and the Tm value chosen to classify positive from negative marked by dotted line (bottom). Both graphs correspond to a concentration of 458 genomes of *L. monocytogenes* per chip. **(C)** U-dHRM dilution series of *L. monocytogenes* with U-dHRM measured values plotted against spectrometer measured values for DNA content. The sample mean and sample standard deviation are shown. **(D)** In blue: qPCR melt curve generated from a 1:1 mix of 20 ng total DNA input of *S. pneumoniae* and *L. monocytogenes*. In red: qPCR melt curve generated from a 1:1 mix of 0.02 ng total DNA input of *S. pneumoniae* and *L. monocytogenes*. This concentration and reaction mixture is similar to that used for digital chip experiments. In grey: qPCR melt curve generated from a negative template control (NTC) with no bacterial DNA added. **(E)** U-dHRM and OVO SVM classification of *L. monocytogenes* and *S. pneumoniae* in two distinct mixture compositions, demonstrating polymicrobial detection capability. Table 3 shows enumeration of detected curves in panel E.

3.2.3 Absolute Quantification of Bacterial DNA

Digital quantitative power relies on the ability to specifically identify true

positive amplification from non-specific background amplification. To assess

the absolute quantitative power of our platform, we compared U-dHRM melt

curve quantification to intercalating dye-based endpoint dPCR quantification. A

chip was loaded with a monomicrobial DNA sample of *L.*

monocytogenes according to the concentrations described in the lower panel

of Table 2 and U-dHRM was conducted. Then, true positive amplification was

quantified two ways. For the first quantification method, we followed the typical

endpoint PCR enumeration approach (top graph in Fig. 7B), which is based on

measuring the fluorescence of all wells at room temperature, fitting the

distribution of well fluorescence values to a probability density function (PDF),

and applying a fluorescence threshold that best separates the high intensity

population (positive) from the low intensity population (negative). For the

second method, we used our U-dHRM melt curve readout to identify the

number of digital reactions having specific bacterial melt curves. The Tm for a

bacterial amplicon, 1,000 bp long, was expected to be centered at 86.5 °C,

based on data collected from the overloaded training chips (Fig. 7A). To

automate identification of reactions that specifically generated bacterial melt

curves, we fit a PDF to the distribution of individual reaction Tm values and

applied a fluorescence threshold that best separated the high Tm population

(positive, specific amplification) from the low Tm population (non-specific or

negative for amplification), shown in the bottom graph of Fig. 7B. This novel

analysis is uniquely enabled by our platform. The melt curves identified as

positive or negative by this method are shown in Supplementary Fig. 1B and

C, respectively. A no template control (NTC) sample was also run on a

separate chip to characterize the Tm of non-specific amplification products.

The Tm of the NTC chip reactions were significantly lower than the Tm of the

1,000 bp amplicon (Supplementary Fig. 1). Comparable NTC reactions carried

out in a qPCR format generated a non-sense amplicon that is 200 bp or less

(data not shown). This amplicon size difference is likely the reason for the

significant difference in melt curve Tm between the NTC and true positive

reactions. The results of the typical dPCR enumeration method and our novel

melt curve enumeration method were then compared by direct visual

observation (manual analysis) of the reactions. Visual melt curve observation

is used frequently after qPCR to determine whether an amplification reaction

was specific or non-specific. This analysis showed that the dPCR enumeration

approach gave a Type I (false positive identification of reactions having non-

specific melt curves) error rate of 22.6% and Type II (false negative

identification of reactions having bacteria-specific melt curves) error rate of

1.19% (average across 3 chips), resulting in a lower limit of detection of ~238

genomes per chip. Our automated melt curve enumeration method based on

Tm gave Type I and II error rates of 0.07% and 0.00%, respectively (average

across 3 chips) compared to manual analysis, which enables a single copy

detection limit. This suggests that our platform could enable general intercalating dye-based dPCR quantification to perform more reliably, even for difficult-to-optimize or partially inhibited reactions that can occur with clinical samples. We then analyzed a ten-fold dilution series of monomicrobial DNA samples of *L. monocytogenes* on-chip using the melt curve enumeration method of Tm thresholding. This showed a linear relationship across the monomicrobial DNA dilution series having an r^2 value of 1 and high measurement precision demonstrated by the low sample standard deviations at each dilution (Fig. 7C).

Next, we compared the number of curves quantified by our melt curve Tm enumeration method with the sample DNA concentrations calculated from spectrometer readings and qPCR standard curve methods (Supplementary Fig. 2). Table 2 shows that our U-dHRM platform and melt curve enumeration method detects *total* DNA concentrations at similar levels as the other two technologies. However, our approach suggests that U-dHRM is able to distinguish *target* DNA from *background* amplified DNA based on melt curve Tm.

Table 2: Comparison of Genomic DNA Quantification Techniques
The concentration of genomic DNA isolated from both *S. pneumoniae* and *L. monocytogenes* was measured using an Eppendorf Biospectrometer, by qPCR standard curve method, and using U-dHRM. Total U-dHRM values are the sum of reactions identified as having specific amplification of bacterial DNA plus the reactions having off-target amplification. Reactions having no amplification, i.e. no melt curve, were classified as true negatives and make up the remainder of the 20,000 total reactions per U-dHRM chip (not represented in this table). QPCR standard curves are shown in Suppl. Fig. 2. Absorbance measurements were made on stock DNA, then the DNA was serially diluted. The calculated concentration of the dilution used on chip is reported here for each measurement modality.

Bacteria	Method of Quantification	Number of Genomes/μL
S. pneumoniae	Absorbance	5780
	qPCR	6554
	U-dHRM total	5460
	bacterial melt curves	1200
	non-template melt curves	4260
L. monocytogenes	Absorbance	9160
	qPCR	10839
	U-dHRM total	7580
	bacterial melt curves	2260
	non-template melt curves	5320

3.2.4 Identification and Quantification in Polymicrobial Samples

To begin to test the specificity and breadth of profiling of our U-dHRM platform, mock polymicrobial samples were generated to represent challenging detection scenarios where one organism vastly outnumbers another. Defined mixtures of *S. pneumoniae* and *L. monocytogenes* DNA were prepared at two different ratios, 1:1 and 3:1, respectively (Table 3). These mixtures were applied separately to two chips at concentrations nearing the

low and high end of a typical clinical pathogen load for neonatal bacteremia (50–2,000 copies). Importantly, this dynamic range cannot be assessed by any current HRM format (Fig. 4A). The heterogeneous samples were subjected to U-dHRM followed by automated Tm thresholding for true-positives and subsequent OVOSVM analysis. Figure 7E shows the OVO SVM identified melt curves for the 1:1 and 1:3 ratios, respectively. Yellow melt curves represent those identified as *L. monocytogenes* and blue as *S. pneumoniae*. Table 3 displays the bacterial composition of the sample reported by the OVO SVM output, i.e. total number of curves classified into each bacterial identity category. The same 1:1 mixture was analyzed by qPCR HRM for comparison, (Fig. 7D). Bulk qPCR HRM fails to indicate the presence of two distinct bacterial species (blue curve) or, in cases of very low DNA input, the presence of any bacteria at all (red curve) due to overwhelming background amplification that results in a melt curve matching the NTC melt curve. This is a common problem for PCR reactions involving universal bacterial primers, since fragments of contaminating bacterial DNA are often present in reagents and liquid handling disposables[183,184]. Extensive pre-treatment of all reagents and supplies with DNase can help to improve this. However, contamination of the actual sample cannot be dealt with in the same way, and must be overcome by the detection methodology.

Table 3: OVO SVM Classification of Mixed Genomic DNA Samples
DPCR chips were loaded with polymicrobial samples containing different proportions (ratios) of *S. pneumoniae* DNA to *L. monocytogenes* DNA to mimic challenging detection scenarios where one organism dominates a test sample. The targeted mixture ratios were created based on absorbance measurements of individual bacterial DNA concentrations using an Eppendorf Biospectrometer and then analyzed by U-dHRM and OVO SVM classification.

| Experiment | Species Mixture | Absorbance | | U-dHRM | |
		Targeted Ratio of Genomes	Estimated Number of Genomes Added to Chip	Measured Number of Genomes On-Chip	Measured Ratio of Genomes
1	*S. pneumoniae*		289	60	
	L. monocytogenes	1:1	458	113	1: 1.88
2	*S. pneumoniae*		1445	238	
	L. monocytogenes	3:1	458	119	2:1

3.2.5 Detection and Quantification of Microbial DNA in Mock Clinical Samples

A mock experiment was conducted to test whether the large amount of human DNA associated with a clinical blood sample would inhibit U-dHRM pathogen identification. Human DNA, extracted directly from a clinical blood sample of a healthy patient, was mixed with DNA from *L. monocytogene*s in the range of a typical pathogen load (<2,000 bacterial genomes/ml blood). This mixture was loaded onto the chip and U-dHRM was performed using our integrated platform. A Tm threshold value was calculated (Fig. 8A) for separating reactions positive for bacterial amplicons (Fig. 8B) from negative

reactions (Fig. 8C). This Tm threshold was higher than the one calculated

previously for bacteria-only samples due to a distinct background amplification

profile, presumably originating from the human DNA. Human DNA background

was associated with more noise in non-specific melt curves, as shown in Fig.

8C, compared to samples that did not include human DNA (Supplementary

Fig. 1C). This higher level of noise resulted in slight adjustments to the

threshold values used to delineate background from true melt curves (Fig. 8B

and C, also see Methods). Nonetheless, 121 *L. monocytogenes* genomes per

20,000 reactions were identified. Figure 8D shows the bacterial melt curves

identified in the mock clinical sample by our U-dHRM platform with automated

analyses.
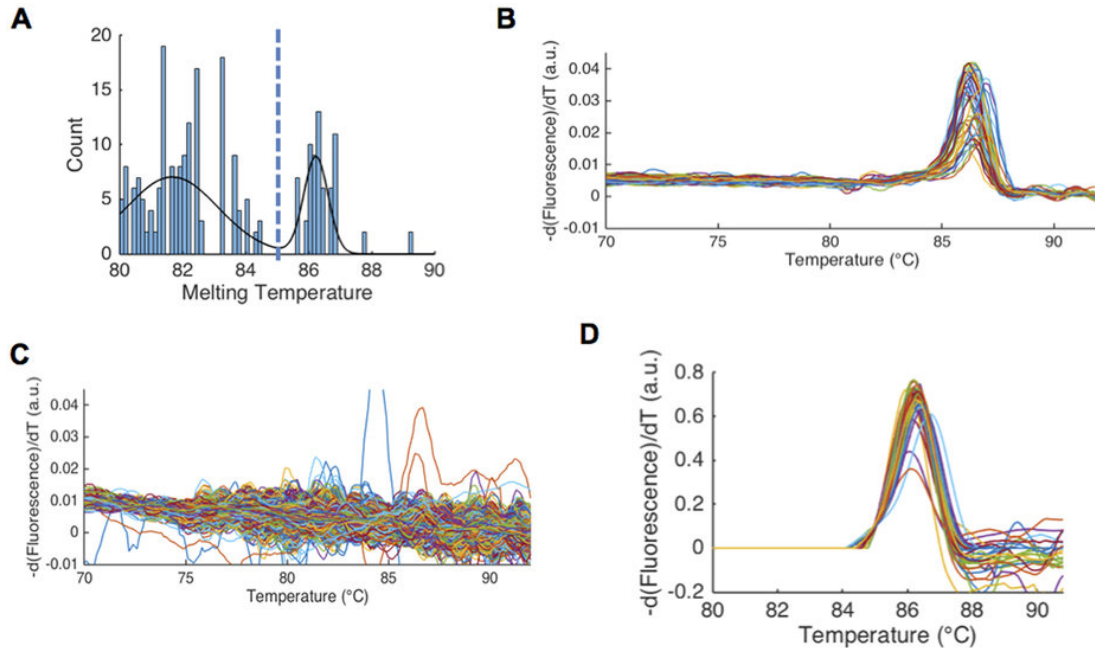
Figure 8: Identification of *L. monocytogenes* in mock blood sample.
(A) Histogram showing the Tm of each digital reaction with PDF overlay and the calculated Tm threshold (dotted line) used to classify true positive from off-target amplification. **(B)** Bacterial DNA melt curves from reactions identified as positive using the Tm and peak height thresholds adjusted for human DNA background. **(C)** Melt curves from reactions identified as negative using thresholds specific for human DNA background. This plot highlights the high background noise associated with the addition of human DNA to our sample **(D)** *L. monocytogenes* melt curves from panel B normalized and aligned to $0.1 - dF/dT$.

3.3 Discussion

Our integrative U-dHRM platform advances HRM profiling by enabling the absolute quantification and identification of multiple genotypes in heterogeneous samples and at clinically relevant concentrations. By achieving HRM curve generation in 0.005% of the traditional HRM volume, and by massive parallelization of HRM across 20,000 reactions simultaneously, we achieve over a 200-fold increase in the dynamic range of detection compared to current HRM formats. Reduction in the size of reactions allows smaller volumes of reagents to be used while maintaining optimal reagent concentrations. Partitioning heterogeneous mixtures across 20,000 picoliter-scale reactions is also expected to overcome environmental microbial DNA contamination that may occur in real-world samples by spatially diluting, i.e. contaminating DNA and target DNA are partitioned from each other for discrimination and quantification[115]. An increased number of reactions also permits rapid generation of a large training curve database for each organism. Incorporating reference temperature calibrator sequences into each reaction helps normalizes against reaction condition variations for improved reliability. Automated melt curve identification is accomplished by removing non-specific melt curves by Tm thresholding and subsequently matching the remaining melt curves to a training database using our OVO SVM machine learning algorithm[173,175]. Together, these approaches comprise our microfluidic U-

dHRM system and enable the quantitative characterization of complex samples containing multiple bacterial organisms.

Intercalating dye-based dPCR is typically used to detect a single, specific amplification product from one bacteria. Probe-based dPCR can be used to specifically identify up to four bacteria by multiplexing fluorescent probes, or a universal probe can be designed to detect the presence of bacteria non-specifically. By incorporating HRM and universal amplification into dPCR, our platform enables probe-free differentiation of multiple bacteria in a single sample. In our previous work, we showed that 37 clinically relevant organisms could be distinguished by general intercalating dye-based melt curves[173]. We anticipate that our U-dHRM platform will achieve at least this level of multiplexing and potentially more, since we were able to accomplish a signal to noise ratio and temperature resolution on-chip that matched standard qPCR HRM machines.

While a direct comparison of our U-dHRM detection method to a universal probe-based dPCR detection method was not feasible, due to different polymerase and reaction chemistry requirements, a comparison to typical intercalating dye-based dPCR techniques suggested that our platform and automated analysis approach may offer specificity and sensitivity improvements. Standard intercalating dye-based dPCR relies on thresholding total fluorescence intensity of digital reactions to determine whether they are positive or negative for amplification. Inhibitors that reduce amplification

efficiency or non-specific background amplification could result in fluorescence intensities that are misclassified, giving rise to false positives and false negatives. However, melt curve analysis may offer a more reliable way to resolve these two conditions. For our reaction chemistry, we found that the typical dPCR approach of applying an intensity threshold to remove false positives left a significant number of reactions misclassified. Bacteria-specific melt curves were observed in several reactions classified as negative by this technique, and non-specific melt curves were observed in several reactions classified as positive. Our platform enabled Tm thresholding, which improved accuracy by 99% and 94%, respectively, in the Type I and II error rates based on manual observation of melt curves. Our approach could help to ensure that true single molecule sensitivity is attained for optimal lower limit of detection. One reason dPCR total fluorescence thresholding performed poorly in our study could be that we thermocycled significantly longer than most dPCR protocols recommend. A typical dPCR cycle number is kept to ~35, but we find that 70 cycles ensures full endpoint amplification from single molecules[115]. While this extended cycling improves accuracy of single-molecule target detection, it also allows off-target amplification to fluoresce more prominently in negative reactions.

Indeed, U-dHRM experiments showed evidence of two kinds of non-template amplification: non-template bacterial DNA amplification (contamination) and off-target amplification. Bacterial contamination produced

distinct melt curves within the Tm range of 84–90 °C (Suppl Fig. 1C). Given

their high Tm, these melt curves are only likely to arise from amplification of

the bacterial 16S gene long amplicon (~1 kbp). Sources of bacterial PCR

contamination, which broad-based 16S amplification is highly sensitive to,

include molecular biology grade water, PCR reagents, the environment, and

DNA extraction kits[185]. Many studies have identified DNA polymerase

preparations as the primary source of PCR contamination. The contamination

of commercially available polymerase preparations is estimated at 10–1000

genomes/U enzyme[186]. Thus for our system, we would expect between 2.9

and 290 contaminating bacterial genomes per reaction, which is consistent

with our observations (Suppl. Fig. 1C).

Off-target amplicons were observed to melt at lower temperatures

(Suppl. Figs 1C and 4D, Tm of ~81 °C). In U-dHRM, these products only arose

in wells that were negative for bacterial DNA (Suppl. Fig. 1B and C). In qPCR,

this off-target product was present in low-template and water control reactions

and out-competed bacterial DNA in these conditions (Fig. 7D and Suppl. Fig.

3). Based on Sanger sequencing analysis, this amplification product was non-

specific (data not shown) and ~150 bp long by gel electrophoresis analysis

(Suppl. Fig. 3). Low reaction efficiency associated with long amplicon PCR

and increased cycling time likely contributed to this non-specific amplification.

An amplicon size <200 bp is ideal for qPCR. However, our goal is to

discriminate numerous bacteria by their 16S sequences, where

hypervariability occurs over ~1 kbp. Thus, for specific bacterial identification,

we require a 1000 bp amplicon, which can reduce qPCR efficiency

significantly[187,188]. In highly efficient qPCR reactions, unintended amplification

products usually amplify at a lower efficiency than that of the target, and so are

out-competed. However, long amplicon targets suffer from low amplification

efficiency[187], allowing off-target amplification to more readily overtake target

amplification when the amount of template is relatively low. This reduces the

sensitivity of qPCR assays for low-level targets. Our standard curves show

that we experience low amplification efficiency comparable to that reported by

others in the literature (e.g. 60%, Suppl. Fig. 2A)[188]. This explains the poor

sensitivity of qPCR to low target concentrations (Suppl. Fig. 2A).

Importantly, it also highlights a strength of U-dHRM. Because digital reaction

partitioning (1) reduces the effect of inhibitors, (2) reduces the effective

concentration of contaminating DNA molecules that give rise to off-target

amplification, and (3) allows for extended cycling to overcome low efficiency of

amplification, since quantification is an endpoint measurement, it is not

surprising that we achieve greater sensitivity in the dHRM format (Fig. 7C)

than in a qPCR format (Suppl. Fig. 2A). Critically, our integration of HRM with

dPCR allows for detection of target, contaminant, and off-target amplification

products, and our OVO SVM approach for melt curve signature identification

and quantification enables broad-based, automated identification of bacterial

organisms.

However, some foreseeable limitations exist. Improvements to the temperature ramp reliability will be critical to ensure a larger database of melt curves are reliably resolved by U-dHRM. Here, calibrator sequences were used to align curves for initial Tm thresholding, but subsequently aligned to their derivative fluorescence value of 0.1 for shape comparison. This second alignment had the effect of ignoring Tm differences in bacteria-specific amplicons, and was required due to fluctuations in the temperature ramp from run-to-run. Insulation from environmental temperatures, an improved chip design with lower thermal mass, and incorporation of a PID controller are expected to overcome this issue. These improvements could also to lead to reduced background noise in the melt curve signal. This would improve our ability to resolve small changes in melt curve shapes generated on the U-dHRM platform, which are occasionally removed by our curve processing algorithms due to background noise.

The capabilities of our microfluidic U-dHRM system could impact infectious disease detection applications like neonatal bacteremia, where speed, breadth of detection, and sensitivity are critical factors. Clinical microbiology relies on lengthy culture-based assays to diagnose bacteremia, which has a high mortality rate that increases with every hour a patient goes undiagnosed and imprecisely treated. Polymicrobial bacteremia is associated with an even higher mortality rate than monomicrobial infection, highlighting the need to detect multiple organisms sensitively, and simultaneously.

Immediate conservative treatment with broad-spectrum intravenous antibiotic therapy is typically initiated without any diagnostic information, leading to inaccurate and overtreatment as well as misuse of multiple antibiotics giving rise to the emergence of drug resistant pathogens. The ability to identify bacterial organisms in a blood sample within hours could change clinical practice by providing diagnostic information in time to alter treatment decisions. Retrospective studies also suggest that absolute quantification of bacterial genomic load in patients may be useful to assess severity of infection and to predict prognosis[4]. The detection of microbial DNA in clinical samples is typically challenged by the excess of human DNA compared to pathogen DNA, which can contribute to PCR reaction inhibition[30,65,155,189]. DPCR has been shown to decrease the impact of inhibitory substances[190]. Likewise, we find that U-dHRM detection of microbial DNA in mock blood samples is not inhibited by high human DNA background or inhibitors carried over in the DNA extraction from blood. This suggests that our device could have exciting implications in the clinical setting. Future work will focus on optimizing and validating our U-dHRM technology on patient-derived clinical samples.

Finally, computational approaches for anomaly detection are being explored by our group to identify bacterial melt curves that are not represented in our database. Currently, a 16S amplicon that melts above the Tm threshold will be automatically classified by our OVO SVM as the organism to which the melt curve is most closely matched. For undefined samples, where

significantly more organisms may arise and unexpected emerging pathogens could be present, it will be crucial to identify whether a melt curve is a poor match to the database curves. Indeed, other groups have discovered new species of bacteria by observing alterations in bulk HRM curves by eye[178]. Automation of this ability would represent a significant advancement for HRM profiling technology and is under development by our group.

3.4 Methods

3.4.1 High-Content U-dHRM Chip

In order to achieve high-content digital partitioning, the sample is loaded into a commercially available QuantStudio 3D Digital PCR 20 K Chip v2 (Applied Biosystems, Foster City, CA). The chip contains 20,000 picoliter-scale wells manufactured from silicon with a hydrophilic treatment that allows high efficiency sample loading. A PCR-grade oil is deposited onto the loaded chip to prevent sample evaporation during cycling. The chip is sealed with an adhesive lid containing an optical window, which allows for imaging and the generation of melt curves. We chose to use a commercially manufactured chip for performance reliability. We coupled the dPCR chip to our custom designed master mix. The master mix is optimized to consistently amplify full length ~1,000 bp templates of the 16S gene, hypervariable regions V1-V6, and produce high fluorescence signal intensity for melt curve analysis while maintaining optimal surface tension for easy loading. An MJ Research PTC-

200 Thermal Cycler (MJ Research Waltham, MA) is used for endpoint

amplification. The thermal cycler is tilted at a 30-degree angle to collect the

bubbles generated at high temperatures in the PCR-oil. These bubbles are

trapped in an air pocket located outside of the chip's sample region,

preventing sample evaporation from the small volume reactions.

3.4.2 Bacterial DNA Isolation and PCR

Wizard Genomic DNA Purification Kit (Promega Corporation, Madison,

WI) was used to isolate DNA from an overnight culture of bacteria, and diluted

in PCR water to the desired concentration. Absorbance measurements were

made on stock DNA at concentrations within the working range of the

spectrophotometer. Then, the DNA was serially diluted, and the expected

concentration of the dilution used for dHRM was reported in the Tables and

Figures for direct comparison of the different measuring modalities. The

optimum PCR master mix for chip amplification, contained in a 14.5 µL

reaction, was found to be 1X Phusion HF Buffer containing 1.5 mM MgCl2

(Thermo Fisher Scientific, Waltham, MA), 0.15 uM forward primer 5′-

GYGGCGNACGGGTGAGTAA-3′ (Integrated DNA Technologies, Coralville,

IA), 0.15 uM reverse primer 5′-AGCTGACGACANCCATGCA-3′ (Integrated

DNA Technologies, Coralville, IA), 0.2 mM dNTPs (Invitrogen, Carlsbad, CA),

2.5X EvaGreen (Biotium, Freemont, CA), 2X ROX (Thermo Fisher Scientific,

Waltham, MA), 0.02 U/µL of Phusion HotStart Polymerase (Thermo Fisher

Scientific, Waltham, MA), 1 µL of sample, and ultra pure PCR water (Quality

Biological Inc., Gaithersburg, MD) to bring the total volume to 14.5 µL. The

dPCR chip was cycled on a flatbed thermocycler with the following cycle: an

initial enzyme activation (98 °C, 30 s), followed by 70 cycles (95 °C, 30 s, 59 °C,

30 s, 72 °C, 60 s). Temperature calibrator sequences with varying GC content

used for system optimization are as follows: 0% GC

(TTAAATTATAAAATATTTATAATATTAATTATATATATAAATATAATA-C3),

12% GC

(TTAATTATAAAGGTATTTATAATATTGAATTATACATATCTAATATAATC-

C3), and 76% GC

(GCGCGGCCGGCACCCGAGACTCTGAGCGGCTGCTGGAGGTGCGGAAG

CGGAGGGGCGGG-C3)[172].

3.4.3 Chip Heating Device

The U-dHRM device consists of a thermoelectric heating/cooling device

(TE Technology, Unc. Traverse City, MI) controlled via an Arduino-based

interface that uses pulse width modulation (PWM) to generate a temperature

ramp (Fig. 4B and C). The thermoelectric device is in direct contact with a

copper plate onto which the dPCR chips coated with a thin layer of thermal

paste are clamped. This allows for even heat distribution and optimal surface

contact. On the reverse side of the thermoelectric chip, an aluminum heat sink

is attached to enable fast excessive heat dissipation. A type K thermocouple

(OMEGA Engineering, Stamford, CT) is used to measure the temperature for each image taken during the temperature ramping. The thermocouple is fixed inside a surrogate chip, which is attached alongside the sample chip to the copper plate. The temperature readings are acquired by the microscope imaging software (Nikon NIS-Elements) and are embedded in the image file metadata for offline analysis. The complete chip-heating setup is placed in a custom designed 3D printed stage adapter to securely mount the device on the microscope for imaging.

3.4.4 Fluorescent Imaging

Fluorescent imaging is accomplished using a Nikon Eclipse Ti platform customized for our dHRM system. A Nikon Plan/Fluor 4X objective with a numerical aperture of 0.13 and a working distance of 16.5X minimizes the number of images and time required to scan the entire chip. A Lumencor SPECTRA X LED Light Engine capable of producing 3–4 W of visible light from 380 nm to 680 nm is used as a light source. Images of the loading control dye, ROX, and melt curve intercalating dye, EvaGreen, are captured with 488/561 nm and 405/488 nm excitation/emission filters using an exposure time of 100 milliseconds. Images are captured every five seconds using a Hamamatsu digital camera, C11440 ORCA-Flash4.0. NIS-Elements software is programmed to automatically image the chip as the heating device ramps using the following workflow: define the capture settings for the ROX and

EvaGreen channels, set the stage area to the chip's sample area, generate

points within that stage area to image, and run time lapse to image each

location for every time point. A Prior Scientific NanoScanZ (Rockland, MA)

motorized stage is used to scan and image the entire chip automatically via

the software. For every image, the microscope automatically records the

temperature registered by our temperature probe within the metadata of the

image. This allows for continuous scanning of the chip and recording of the

fluorescence intensity in each well while concurrently heating the chip to

generate 20,000 melt curves.

3.4.5 Image analysis and SVM

3.4.5.1 Fluorescence and Tm thresholding for negative reaction removal

Two approaches to thresholding reaction fluorescence for the

identification and removal of negative reactions were compared. The typical

dPCR approach of thresholding total reaction fluorescence was accomplished

by first plotting a histogram in MATLAB of the total fluorescence intensities at

room temperature of all chip reactions. The probability density function (PDF)

for a mixture of two normal distributions was then applied to identify negative

and positive reaction distributions. A threshold was identified at the lowest

point of intensity where the two distributions intersected (Fig. 7B, top). This

was performed for each sample type (i.e. DNA extracted from pure bacterial

culture versus mock blood sample) to identify the appropriate threshold given unique background distributions.

A second approach was developed to identify a Tm threshold that separated off-target amplified reactions from true positives more accurately. First, raw melt curves were converted to derivative melt curves. On fully loaded chips where all reactions were positive (2 training chips) all reactions contained 16S amplicons, which were observed to melt with an average Tm of 89 °C. On digitized chips (3 chips, testing data), off-target amplicons were observed to melt at much lower temperatures, average Tm of 81 °C, while positive 16S amplicons melted reproducibly in the same range as the training chips. For thresholding analysis, the maximum peak height (Tm) above $-d(Fluorescence)/dT = 0.01$ was found for each derivative melt curve between the range of 75 °C and 93 °C. Then a histogram of the Tms was plotted in MATLAB, and the PDF for a mixture of two normal distributions was applied (Fig. 7B, bottom). Finally, the Tm threshold was chosen at the minima between the two distributions. Reactions melting below this Tm threshold were identified as negatives, while those melting above the threshold were identified as positives. The Tm threshold for samples of DNA extracted from pure bacterial cultures was identified and held constant at 84 °C.

3.4.5.2 Melt curve data generation

In order to generate melt curves from the acquired fluorescent images of the dPCR chip, we implement an automated image processing algorithm in MATLAB. The algorithm generates a binary mask for each temperature point to identify the centroid corresponding to each digital reaction well in the field. Then records the pixel intensity of the 441 neighboring pixels from the images of both the EvaGreen channel and the ROX channel. Each well's average pixel intensity is plotted against the measured temperature to generate the raw melt curve. Each melt curve is normalized to the ROX channel to account for any differences due to unequal loading. The Tm threshold described above is then applied to remove negative reactions and all incorrectly identified centroids. A Gaussian filter is then used to smooth the curves and the derivative is taken with respect to temperature to obtain –dF/dT. Finally, the curves are aligned via a temperature independent melt curve alignment at 0.1 –dF/dT. This allowed the differences in melt curve shape to be maximized for later identification using a previously developed OVO SVM algorithm[173]. Briefly, an OVO SVM creates a maximal margin separating hyperplane between two data classes (i.e. melt curve signatures) using the Least Squares Method (linear kernel). OVO SVMs were created for all binary combinations of organisms with the training data generated from melt curves of known origin. During classification, a scoring method is applied and the most frequently called classification is chosen as the final melt curve identity.

3.4.6 Clinical Blood Sample Purification and Analysis

DNA from a clinical blood sample, which was known to be negative for bacterial infection, was extracted and purified using a High Pure PCR Template Preparation Kit (Roche Diagnostics Corporation, Indianapolis, IN). The purified blood DNA was eluted in a 20 µL volume. DNA of *L. monocytogenes* was isolated using the protocol described above in the methods section. Approximately 2,000 genomes of *L. monocytogenes* were added to the purified blood extraction. The maximum amount of the blood and bacterial DNA mixture (8.63 µL) was added to the PCR master mix. The final mass ratio of human DNA to bacterial DNA on chip was 12,172:1. The master mix was then loaded onto the chip and U-dHRM was performed following 70 amplification cycles. The full chip was imaged as four tiles. Changes were made to the Tm thresholding script to account for the increased and oscillatory noise introduced by the blood DNA extract. First, the peak height for the derivative melt curve was raised to $-dF/dT = 0.015$ to threshold noisier non-specific melt curves from true bacterial amplicons. Second, a lower threshold for melt curve troughs was added at $-0.004 -dF/dT$, which aided in removing highly oscillatory and anomalous curves.

3.4.7 Cell Culture

Clinically isolated *S. pneumoniae* and *L. monocytogenes* were grown separately overnight in Luria-Bertani (LB) broth. Sterile conditions were used to ensure uncontaminated growth of each bacteria.

Chapter 3, in full, is a reprint of the material as it appears in Scientific Reports 2017. Velez Ortiz, Daniel; Mack, Hannah; Jupe, Julietta; Hawker, Sinead; Kulkarni, Ninad; Hedayatnia, Behnam; Zhang, Yang; Lawrence, Shelley; Fraley, Stephanie I. Macmillan Publishers Limited, 2017. The thesis author was a researcher and co-author of this material. She assisted in developing the experimental procedure and conducted the experiment with the mock blood sample. She also generated Figure 8 and did the final edits of the text for submission.

CHAPTER 4: HARDWARE OPTIMIZATION

Previously, an Arduino was used to control the heating of the device.

Any variability in the environment or starting temperature would affect the heat

ramp. Consistent heating was vital to our system, which relies on temperature-

dependent melt curves being identified by a machine learning algorithm.

Heating differences between runs could affect where and how the bacterial

DNA melts along the temperature axis of our –dF/dT melt plots. A feedback

controller was implemented and optimized to provide repeatable controlled

heating. A temperature sensor was installed in the center of the copper block

between the thermoelectric device (Peltier chip) and the imaging and dummy

chips. This temperature provided real-time feedback which the controller used

to adjust the ramp rate accordingly. Two different controllers (Meerstetter,

TEC-1089-SV and TEC-1122-SV) were tuned and optimized. The controllers

were auto-tuned once a day at 98°C and then cooled to 22°C. During each

run, the device was heated from room temperature to 45°C, stabilized at 45°C

and then ramped 45-98°C at a ramp rate of 0.1°C/s. Simultaneous heating

and imaging is initiated at 45°C and carried out to 98°C; a low temperature

calibrator, which melts around 59°C, is used as a control to account for

potential bacterial melt curve peak shifts and to ensure the chip is heated

uniformly; the long bacterial amplicon completes its melting process by 98°C.

The stability and repeatability of the heat ramp was improved significantly with

the use of the feedback controller; figure 9 shows that a maximum error of

0.005°C was achieved over multiple days using two separate controllers.

Figure 10 displays estimates of the temperature profile at the center of the

chip. The temperature profile of a single run and the repeatability between

runs was significantly improved. With the use of the Arduino, the slope of the

ramp would vary between runs at the higher temperatures where the bacterial

DNA melts. These slope differences caused the same DNA to appear to melt

at slightly different temperatures. The ramp and imaging rates of the system

are currently being optimized in the digital format to determine if sequence

resolution can be enhanced further.
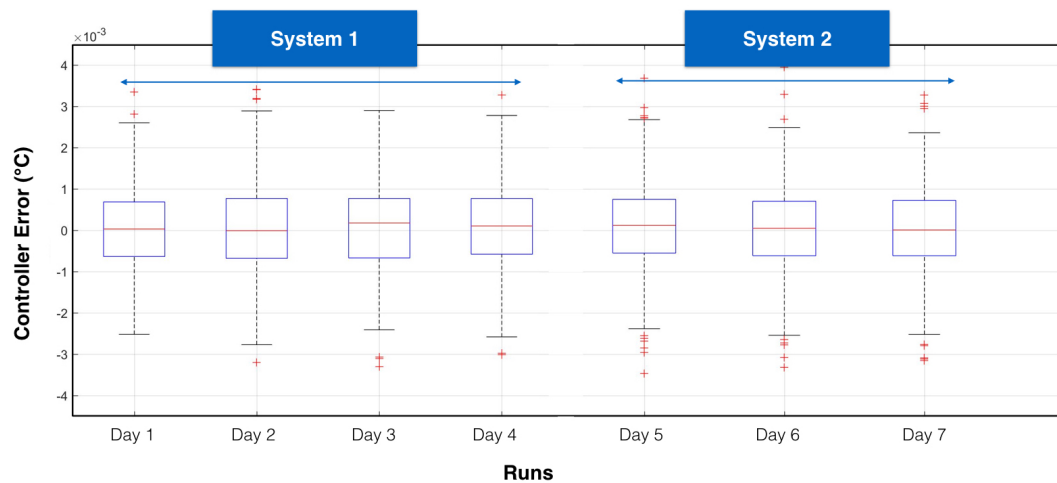
Figure 9: System error characterization across days with two standalone systems
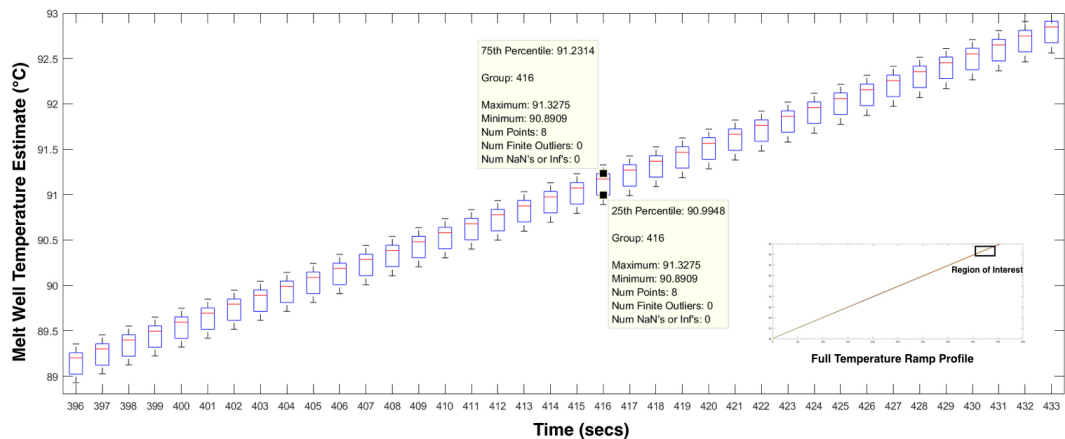
Figure 10: Melt well temperature profile in region of interest (~88-93°C)

CHAPTER 5: CONCLUSION

Sepsis is a life-threatening condition where a patient's mortality rate increases with every hour of incorrect diagnosis or treatment. Rapid and accurate diagnostics are essential to patient survival. The current diagnostic method of blood culture is far from ideal. The ideal sepsis diagnostic should be: (a) rapid, (b) broad-based, (c) capable of polymicrobial detection, (d) highly sensitive and specific, (e) minimally invasive, (f) easily integrated into clinical workflow, (g) able to detect antibiotic resistance determinants, (h) and able to identify new and unknown pathogens. New technologies have been developed to address the problems of blood culture; however, they have not yet achieved all of these ideal characteristics. We have developed the proof-of-principal U-dHRM platform to address this need and have improved its reliability towards future clinical testing and validation; this technology can include all the characteristics of an ideal sepsis diagnostic. Preliminary testing shows that it is currently able to identify 37 sepsis-causing bacteria in a 1 mL blood sample within four hours with single-cell sensitivity and 99.9% specificity. With further optimization, the detection time could be improved to meet the clinically relevant time frame of 1-3 hours. By using a microfluidic chip containing 20,000 reaction wells, each genome of bacteria is separated from one another, allowing for detection of polymicrobial samples. Future work will include development of an anomaly detection algorithm, which would identify

melt curves that are not in the library as novel pathogens. This would allow for the detection and further testing of new and unknown pathogens.

Before this device can be made available for clinical use, a clinical validation study must be conducted; we have shown proof-of-concept using a mock blood sample, but further optimization is required for real clinical samples. Ideally, in the future, the lysis and nucleic acid extraction would be automated by a readily available sample preparation system, such as Roche's MagNA Pure System. Universal primers for viruses and fungi could also be multiplexed so all sepsis-causing pathogens could be determined in a single test; such primers have been previously used in the HRM platform, but they have not been tested and optimized for the digital format.

REFRENCES

1.   Coburn, B., Morris, A. M., Tomlinson, G. & Detsky, A. S. Does this adult
        patient with suspected bacteremia require blood cultures? *JAMA* **308,**
        502–11 (2012).

2.   Bates, D. W., Cook, E. F., Goldman, L. & Lee, T. H. Predicting
        bacteremia in hospitalized patients. A prospectively validated model.
        Ann. Intern. Med. **113,** 495–500 (1990).

3.   Roth, A., Wiklund, A. E., Pålsson, A. S., Melander, E. Z., Wullt, M.,
        Cronqvist, J., Walder, M. & Sturegård, E. Reducing blood culture
        contamination by a simple informational intervention. *J. Clin. Microbiol.*
        48, 4552–8 (2010).

4.   Stryjewski, M. E., Kanafani, Z. A., Chu, V. H., Pappas, P. A., Harding,
        T., Drew, L. A., Benjamin, D. K., Reller, L. B., Lee, B. A., Corey, G. R. &
        Fowler, V. G. Staphylococcus aureus bacteremia among patients with
        health care-associated fever. *Am. J. Med.* **122,** 281–289.e2 (2009).

5.   Buehler, S. S., Madison, B., Snyder, S. R., Derzon, J. H., Cornish, N. E.,
        Saubolle, M. A., Weissfeld, A. S., Weinstein, M. P., Liebow, E. B. &
        Wolk, D. M. Effectiveness of Practices To Increase Timeliness of
        Providing Targeted Therapy for Inpatients with Bloodstream Infections: a
        Laboratory Medicine Best Practices Systematic Review and Meta-
        analysis. *Clin. Microbiol. Rev.* **29,** 59–103 (2016).

6.   Epstein, L., Dantes, R., Magill, S. & Fiore, A. Varying Estimates of
        Sepsis Mortality Using Death Certificates and Administrative Codes--
        United States, 1999-2014. *MMWR. Morb. Mortal. Wkly. Rep.* **65,** 342–
        345 (2016).

7.   Weinstein, M. P., Murphy, J. R., Reller, L. B. & Lichtenstein, K. A. The
        clinical significance of positive blood cultures: a comprehensive analysis
        of 500 episodes of bacteremia and fungemia in adults. II. Clinical
        observations, with special reference to factors influencing prognosis.
        Rev. Infect. Dis. **5,** 54–70 (1983).

8.   Lee, C.-C., Chen, S.-Y., Chang, I.-J., Chen, S.-C. & Wu, S.-C.
        Comparison of clinical manifestations and outcome of community-
        acquired bloodstream infections among the oldest old, elderly, and adult
        patients. *Medicine (Baltimore).* **86,** 138–144 (2007).

9.   Weinstein, M. P., Towns, M. L., Quartey, S. M., Mirrett, S., Reimer, L.
        G., Parmigiani, G. & Reller, L. B. The clinical significance of positive

blood cultures in the 1990s: a prospective comprehensive evaluation of the microbiology, epidemiology, and outcome of bacteremia and fungemia in adults. *Clin. Infect. Dis.* **24,** 584–602 (1997).

10. Klevens, R. M., Edwards, J. R. & Gaynes, R. P. The impact of antimicrobial-resistant, health care-associated infections on mortality in the United States. *Clin. Infect. Dis.* **47,** 927–930 (2008).

11. Elixhauser, A., Friedman, B. & Stranges, E. Septicemia in US hospitals, 2009. *Agency Healthc. Res. Qual.* **348,** 1–13 (2011).

12. Novosad, S. A., Sapiano, M. R. P., Grigg, C., Lake, J., Robyn, M., Dumyati, G., Felsen, C., Blog, D., Dufort, E., Zansky, S., Wiedeman, K., Avery, L., Dantes, R. B., Jernigan, J. A., Magill, S. S., Fiore, A. & Epstein, L. Vital Signs: Epidemiology of Sepsis: Prevalence of Health Care Factors and Opportunities for Prevention. *MMWR. Morb. Mortal. Wkly. Rep.* **65,** 864–869 (2016).

13. Torio, C. M. & Moore, B. J. National Inpatient Hospital Costs: The Most Expensive Conditions by Pay, 2011. **204,** 1–15 (2016).

14. Kiser, C., Nawab, U., McKenna, K. & Aghai, Z. H. Role of guidelines on length of therapy in chorioamnionitis and neonatal sepsis. *Pediatrics* **133,** 992–998 (2014).

15. Patel, S. J. & Saiman, L. Principles and strategies of antimicrobial stewardship in the neonatal intensive care unit. *Semin. Perinatol.* **36,** 431–436 (2012).

16. Heron M. Infant, neonatal, and postnatal deaths, percentage of total deaths, and mortality rates for the 10 leading causes of infant death, by race and sex:United States, 2010. *Natl. Vital Stat. Reports* **December 6,** Table 3 (2013).

17. Tripathi, N., Cotten, C. M. & Smith, P. B. Antibiotic use and misuse in the neonatal intensive care unit. *Clin. Perinatol.* **39,** 61–68 (2012).

18. Patel, S. J., Oshodi, A., Prasad, P., Delamora, P., Larson, E., Zaoutis, T., Paul, D. A. & Saiman, L. Antibiotic use in neonatal intensive care units and adherence with Centers for Disease Control and Prevention 12 Step Campaign to Prevent Antimicrobial Resistance. *Pediatr. Infect. Dis. J.* **28,** 1047–1051 (2009).

19. Verani, J. R., McGee, L. & Schrag, S. J. Prevention of perinatal group B streptococcal disease--revised guidelines from CDC, 2010. *MMWR.*

Recomm. Rep. **59,** 1–36 (2010).

20. Storro, O., Avershina, E. & Rudi, K. Diversity of intestinal microbiota in infancy and the risk of allergic disease in childhood. *Curr. Opin. Allergy Clin. Immunol.* **13,** 257–262 (2013).

21. Saari, A., Virta, L. J., Sankilampi, U., Dunkel, L. & Saxen, H. Antibiotic exposure in infancy and risk of being overweight in the first 24 months of life. *Pediatrics* **135,** 617–626 (2015).

22. Blackburn, R. M., Muller-Pebody, B., Planche, T., Johnson, A., Hopkins, S., Sharland, M., Kennea, N. & Heath, P. T. Neonatal sepsis--many blood samples, few positive cultures: implications for improving antibiotic prescribing. *Archives of disease in childhood. Fetal and neonatal edition* **97,** F487-8 (2012).

23. Ottolini, M. C., Lundgren, K., Mirkinson, L. J., Cason, S. & Ottolini, M. G. Utility of complete blood count and blood culture screening to diagnose neonatal sepsis in the asymptomatic at risk newborn. *Pediatr. Infect. Dis. J.* **22,** 430–434 (2003).

24. Weston, E. J., Pondo, T., Lewis, M. M., Martell-Cleary, P., Morin, C., Jewell, B., Daily, P., Apostol, M., Petit, S., Farley, M., Lynfield, R., Reingold, A., Hansen, N. I., Stoll, B. J., Shane, A. L., Zell, E. & Schrag, S. J. The burden of invasive early-onset neonatal sepsis in the United States, 2005-2008. *Pediatr. Infect. Dis. J.* **30,** 937–941 (2011).

25. Edmond, K. & Zaidi, A. New approaches to preventing, diagnosing, and treating neonatal sepsis. *PLoS Med.* **7,** 1–8 (2010).

26. Greenwood, C., Morrow, A. L., Lagomarcino, A. J., Altaye, M., Taft, D. H., Yu, Z., Newburg, D. S., Ward, D. V & Schibler, K. R. Early empiric antibiotic use in preterm infants is associated with lower bacterial diversity and higher relative abundance of Enterobacter. *J. Pediatr.* **165,** 23–29 (2014).

27. Qazi, S. A. & Stoll, B. J. Neonatal sepsis: a major global public health challenge. *Pediatr. Infect. Dis. J.* **28,** S1-2 (2009).

28. Weiss, S. L., Fitzgerald, J. C., Balamuth, F., Alpern, E. R., Lavelle, J., Chilutti, M., Grundmeier, R., Nadkarni, V. M. & Thomas, N. J. Delayed antimicrobial therapy increases mortality and organ dysfunction duration in pediatric sepsis. *Crit. Care Med.* **42,** 2409–2417 (2014).

29. Benitz, W. E. Adjunct laboratory tests in the diagnosis of early-onset

neonatal sepsis. *Clin. Perinatol.* **37,** 421–438 (2010).

30. Dellinger, R. P., Levy, M. M*.,* Carlet, J. M., Bion, J., Parker, M. M., Jaeschke, R., Reinhart, K., Angus, D. C., Brun-Buisson, C., Beale, R., Calandra, T., Dhainaut, J., Gerlach, H., Harvey, M., Marini, J. J., Marshall, J., Ranieri, M., Ramsay, G., Sevransky, J., Thompson, B. T., Townsend, S., Vender, J. S., Zimmerman, J. L., Vincent, J. Surviving Sepsis Campaign: international guidelines for management of severe sepsis and septic shock: 2008. *Intensive Care Med.* **34,** 17–60 (2008).

31. Kollef, M. H., Sherman, G., Ward, S. & Fraser, V. J. Inadequate antimicrobial treatment of infections: a risk factor for hospital mortality among critically ill patients. *Chest* **115,** 462–474 (1999).

32. Garnacho-Montero, J., Garcia-Garmendia, J. L., Barrero-Almodovar, A., Jimenez-Jimenez, F. J., Perez-Paredes, C. & Ortiz-Leyba, C. Impact of adequate empirical antibiotic therapy on the outcome of patients admitted to the intensive care unit with sepsis. *Crit. Care Med.* **31,** 2742–2751 (2003).

33. Valles, J., Rello, J., Ochagavia, A., Garnacho, J. & Alcala, M. A. Community-acquired bloodstream infection in critically ill adult patients: impact of shock and inappropriate antibiotic therapy on survival. *Chest* **123,** 1615–1624 (2003).

34. Blevins, S. M. & Bronze, M. S. Robert Koch and the "golden age" of bacteriology. *Int. J. Infect. Dis.* **14,** e744-51 (2010).

35. Kreger, B. E., Craven, D. E., Carling, P. C. & McCabe, W. R. Gram-negative bacteremia. III. Reassessment of etiology, epidemiology and ecology in 612 patients. *Am. J. Med.* **68,** 332–343 (1980).

36. Bacconi, A., Richmond, G. S., Baroldi, M. A., Laffler, T. G., Blyn, L. B., Carolan, H. E., Frinder, M. R., Toleno, D. M., Metzgar, D., Gutierrez, J. R., Massire, C., Rounds, M., Kennel, N. J., Rothman, R. E., Peterson, S., Carroll, K. C., Wakefield, T., Ecker, D. J., Sampath, R. Improved sensitivity for molecular detection of bacterial and candida infections in blood. *J. Clin. Microbiol.* **52,** 3164–3174 (2014).

37. Opota, O., Jaton, K. & Greub, G. Microbial diagnosis of bloodstream infection: Towards molecular diagnosis directly from blood. *Clin. Microbiol. Infect.* **21,** 323–331 (2015).

38. Cockerill, F. R. 3rd, Wilson, J. W., Vetter, E. A., Goodman, K. M., Torgerson, C. A., Harmsen, W. S., Schleck, C. D., Ilstrup, D. M.,

Washington, J. A. 2nd & Wilson, W. R. Optimal testing parameters for blood cultures. *Clin. Infect. Dis.* **38,** 1724–1730 (2004).

39. Riedel, S., Bourbeau, P., Swartz, B., Brecher, S., Carroll, K. C., Stamper, P. D., Dunne, W. M., McCardle, T., Walk, N., Fiebelkorn, K., Sewell, D., Richter, S. S., Beekmann, S. & Doern, G. V. Timing of specimen collection for blood cultures from febrile patients with bacteremia. *J. Clin. Microbiol.* **46,** 1381–1385 (2008).

40. CLSI document M47-A. Principles and Procedures for Blood Cultures; Aproved Guideline. *Clin. Lab. Standars Inst.* Vol.27 No.17 (2007).

41. Tille, P. *Bailey & Scott's Diagnostic Microbiology.* (Mosby Elsevier, 2015).

42. Garcia, R. A., Spitzer, E. D., Beaudry, J., Beck, C., Diblasi, R., Gilleeny-Blabac, M., Haugaard, C., Heuschneider, S., Kranz, B. P., McLean, K., Morales, K. L., Owens, S., Paciella, M. E. & Torregrosa, E. Multidisciplinary team review of best practices for collection and handling of blood cultures to determine effective interventions for increasing the yield of true-positive bacteremias, reducing contamination, and eliminating false-positive central line-a. *Am. J. Infect. Control* **43,** 1222–1237 (2015).

43. Fenollar, F. & Raoult, D. Molecular diagnosis of bloodstream infections caused by non-cultivable bacteria. *Int. J. Antimicrob. Agents* **30,** 7–15 (2007).

44. Riedel, S. & Carroll, K. C. Blood cultures: key elements for best practices and future directions. *J. Infect. Chemother. Off. J. Japan Soc. Chemother.* **16,** 301–316 (2010).

45. Schrag, S. J., Zell, E. R., Lynfield, R., Roome, A., Arnold, K. E., Craig, A. S., Harrison, L. H., Reingold, A., Stefonek, K., Smith, G., Gamble, M. & Schuchat, A. A population-based comparison of strategies to prevent early-onset group B streptococcal disease in neonates. *N. Engl. J. Med.* **347,** 233–239 (2002).

46. Stoll, B. J., Hansen, N. I., Sánchez, P. J., Faix, R. G., Poindexter, B. B., Van Meurs, K. P., Bizzarro, M. J., Goldberg, R. N., Frantz, I. D., Hale, E. C., Shankaran, S., Kennedy, K., Carlo, W. A., Watterberg, K. L., Bell, E. F., Walsh, M. C., Schibler, K., Laptook, A. R., Shane, A. L., Schrag, S. J., Das, A., Higgins, R. D. Early onset neonatal sepsis: the burden of group B Streptococcal and E. coli disease continues. *Pediatrics* **127,** 817–26 (2011).

47. Cotten, C. M., Taylor, S., Stoll, B., Goldberg, R. N., Hansen, N. I., Sanchez, P. J., Ambalavanan, N. & Benjamin, D. K. J. Prolonged duration of initial empirical antibiotic treatment is associated with increased rates of necrotizing enterocolitis and death for extremely low birth weight infants. *Pediatrics* **123,** 58–66 (2009).

48. Ilstrup, D. M. & Washington, J. A. 2nd. The importance of volume of blood cultured in the detection of bacteremia and fungemia. *Diagn. Microbiol. Infect. Dis.* **1,** 107–110 (1983).

49. Connell, T. G., Rele, M., Cowley, D., Buttery, J. P. & Curtis, N. How reliable is a negative blood culture result? Volume of blood submitted for culture in routine practice in a children's hospital. *Pediatrics* **119,** 891–896 (2007).

50. Mermel, L. A. & Maki, D. G. Detection of bacteremia in adults: consequences of culturing an inadequate volume of blood. *Ann. Intern. Med.* **119,** 270–272 (1993).

51. Dethlefsen, L. & Relman, D. A. Incomplete recovery and individualized responses of the human distal gut microbiota to repeated antibiotic perturbation. *Proc. Natl. Acad. Sci. U. S. A.* **108 Suppl,** 4554–4561 (2011).

52. Bekeris, L. G., Tworek, J. A., Walsh, M. K. & Valenstein, P. N. Trends in blood culture contamination: a College of American Pathologists Q-Tracks study of 356 institutions. *Arch. Pathol. Lab. Med.* **129,** 1222–1225 (2005).

53. Zwang, O. & Albert, R. K. Analysis of strategies to improve cost effectiveness of blood cultures. *J. Hosp. Med.* **1,** 272–276 (2006).

54. Alahmadi, Y. M., Aldeyab, M. A., McElnay, J. C., Scott, M. G., Darwish Elhajji, F. W., Magee, F. A., Dowds, M., Edwards, C., Fullerton, L., Tate, A. & Kearney, M. P. Clinical and economic impact of contaminated blood cultures within the hospital setting. *J. Hosp. Infect.* **77,** 233–236 (2011).

55. Segal, G. S. & Chamberlain, J. M. Resource utilization and contaminated blood cultures in children at risk for occult bacteremia. *Arch. Pediatr. Adolesc. Med.* **154,** 469–473 (2000).

56. Thuler, L. C., Jenicek, M., Turgeon, J. P., Rivard, M., Lebel, P. & Lebel, M. H. Impact of a false positive blood culture result on the management of febrile children. *Pediatr. Infect. Dis. J.* **16,** 846–851 (1997).

57. Gander, R. M., Byrd, L., DeCrescenzo, M., Hirany, S., Bowen, M. & Baughman, J. Impact of blood cultures drawn by phlebotomy on contamination rates and health care costs in a hospital emergency department. *J. Clin. Microbiol.* **47,** 1021–1024 (2009).

58. Pien, B. C., Sundaram, P., Raoof, N., Costa, S. F., Mirrett, S., Woods, C. W., Reller, L. B. & Weinstein, M. P. The clinical and prognostic importance of positive blood cultures in adults. *Am. J. Med.* **123,** 819–828 (2010).

59. Souvenir, D., Anderson, D. E. J., Palpant, S., Mroch, H., Askin, S., Anderson, J., Claridge, J., Eiland, J., Malone, C., Garrison, M. W., Watson, P. & Campbell, D. M. Blood cultures positive for coagulase-negative staphylococci: antisepsis, pseudobacteremia, and therapy of patients. *J. Clin. Microbiol.* **36,** 1923–1926 (1998).

60. Lee, C. C., Lin, W. J., Shih, H. I., Wu, C. J., Chen, P. L., Lee, H. C., Lee, N. Y., Chang, C. M., Wang, L. R. & Ko, W. C. Clinical significance of potential contaminants in blood cultures among patients in a medical center. *J. Microbiol. Immunol. Infect.* **40,** 438–444 (2007).

61. Forrest, G. N., Mankes, K., Jabra-Rizk, M. A., Weekes, E., Johnson, J. K., Lincalis, D. P. & Venezia, R. A. Peptide nucleic acid fluorescence in situ hybridization-based identification of Candida albicans and its impact on mortality and antifungal therapy costs. *J. Clin. Microbiol.* **44,** 3381–3383 (2006).

62. Cunney, R. J., McNamara, E. B., Alansari, N., Loo, B. & Smyth, E. G. The impact of blood culture reporting and clinical liaison on the empiric treatment of bacteraemia. *J. Clin. Pathol.* **50,** 1010–1012 (1997).

63. Zhan, C. & Miller, M. R. Excess length of stay, charges, and mortality attributable to medical injuries during hospitalization. *JAMA* **290,** 1868–1874 (2003).

64. Dunagan, W. C., Woodward, R. S., Medoff, G., Gray, J. L. 3rd, Casabar, E., Smith, M. D., Lawrenz, C. A. & Spitznagel, E. Antimicrobial misuse in patients with positive blood cultures. *Am. J. Med.* **87,** 253–259 (1989).

65. Opota, O., Croxatto, A., Prod'hom, G. & Greub, G. Blood culture-based diagnosis of bacteraemia: state of the art. *Clin. Microbiol. Infect.* **21,** 313–322 (2015).

66. Kothari, A., Morgan, M. & Haake, D. A. Emerging technologies for rapid identification of bloodstream pathogens. *Clin. Infect. Dis.* **59,** 272–278

(2014).

67. Afshari, A., Schrenzel, J., Ieven, M., Harbarth, S. Bench-to-bedside review: Rapid molecular diagnostics for bloodstream infection - a new frontier? *Crit. Care* **16,** 222 (2012).

68. Ecker, D. J., Sampath, R., Li, H., Massire, C., Matthews, H. E., Toleno, D., Hall, T. A., Blyn, L. B., Eshoo, M. W., Ranken, R., Hofstadler, S. A. & Tang, Y. W. New technology for rapid molecular diagnosis of bloodstream infections. *Expert.Rev.Mol.Diagn.* **10,** 399–415 (2010).

69. The IRIDICA Platform. (2017).

70. IRIDICA Technology.

71. Jordana-Lluch, E., Giménez, M., Dolores Quesada, M., Rivaya, B., Marcó, C., Jesus Domínguez, M., Arméstar, F., Martró, E. & Ausina, V. Evaluation of the broad-range PCR/ESI-MS technology in blood specimens for the molecular diagnosis of bloodstream Infections. *PLoS One* **10,** 1–13 (2015).

72. Metzgar, D., Frinder, M. W., Rothman, R. E., Peterson, S., Carroll, K. C., Zhang, S. X., Avornu, G. D., Rounds, M. A., Carolan, H. E., Toleno, D. M., Moore, D., Hall, T. A., Massire, C., Richmond, G. S., Gutierrez, J. R., Sampath, R., Ecker, D. J. & Blyn, L. B. The IRIDICA BAC BSI Assay: Rapid, Sensitive and Culture-Independent Identification of Bacteria and Candida in Blood. *PLoS One* **11,** e0158186 (2016).

73. Vincent, J.-L., Brealey, D., Libert, N., Abidi, N. E., O'Dwyer, M., Zacharowski, K., Mikaszewska-Sokolewicz, M., Schrenzel, J., Simon, F., Wilks, M., Picard-Maureau, M., Chalfin, D. B., Ecker, D. J., Sampath, R. & Singer, M. Rapid Diagnosis of Infection in the Critically Ill, a Multicenter Study of Molecular Detection in Bloodstream Infections, Pneumonia, and Sterile Site Infections. *Crit. Care Med.* **43,** 2283–91 (2015).

74. Desmet, S., Maertens, J., Bueselinck, K. & Lagrou, K. Broad-Range PCR Coupled with Electrospray Ionization Time of Flight Mass Spectrometry for Detection of Bacteremia and Fungemia in Patients with Neutropenic Fever. *J. Clin. Microbiol.* **54,** 2513–20 (2016).

75. Dien Bard, J. & McElvania TeKippe, E. Diagnosis of Bloodstream Infections in Children. *J. Clin. Microbiol.* **54,** JCM.02919-15 (2016).

76. Roche Molecular Diagnostics - IVD Assays and Instruments.

77. Lehmann, L. E., Hunfeld, K.-P., Emrich, T., Haberhausen, G., Wissing, H., Hoeft, A. & Stüber, F. A multiplex real-time PCR assay for rapid detection and differentiation of 25 bacterial and fungal pathogens from whole blood samples. *Med. Microbiol. Immunol.* **197,** 313–324 (2008).

78. Lucignano, B., Ranno, S., Liesenfeld, O., Pizzorno, B., Putignani, L., Bernaschi, P. & Menichella, D. Multiplex PCR Allows Rapid and Accurate Diagnosis of Bloodstream Infections in Newborns and Children with Suspected Sepsis. *J. Clin. Microbiol.* **49,** 2252–2258 (2011).

79. Reers, Y., Idelevich, E. A., Pätkau, H., Sauerland, M. C., Tafelski, S., Nachtigall, I., Berdel, W. E., Peters, G., Silling, G. & Becker, K. Multiplex PCR assay underreports true bloodstream infections with coagulase-negative staphylococci in hematological patients with febrile neutropenia. *Diagn. Microbiol. Infect. Dis.* **85,** 413–415 (2016).

80. Josefson, P., Strålin, K., Ohlin, A., Ennefors, T., Dragsten, B., Andersson, L., Fredlund, H., Mölling, P. & Olcén, P. Evaluation of a commercial multiplex PCR test (SeptiFast) in the etiological diagnosis of community-onset bloodstream infections. *Eur. J. Clin. Microbiol. Infect. Dis.* **30,** 1127–1134 (2011).

81. Dinç, F., Akalin, H., Özakin, C., Sinirtaş, M., Kebabçi, N., Işçimen, R., Kelebek Girgin, N. & Kahveci, F. Comparison of blood culture and multiplex real-time PCR for the diagnosis of nosocomial sepsis. *Minerva Anestesiol.* **82,** 301–9 (2016).

82. Ratzinger, F., Tsirkinidou, I., Haslacher, H., Perkmann, T., Schmetterer, K. G., Mitteregger, D., Makristathis, A. & Burgmann, H. Evaluation of the Septifast MGrade Test on Standard Care Wards—A Cohort Study. *PLoS One* **11,** e0151108 (2016).

83. Dierkes, C., Ehrenstein, B., Siebig, S., Linde, H.-J., Reischl, U. & Salzberger, B. Clinical impact of a commercially available multiplex PCR system for rapid detection of pathogens in patients with presumed sepsis. *BMC Infect. Dis.* **9,** 126 (2009).

84. Dark, P., Blackwood, B., Gates, S., McAuley, D., Perkins, G. D., McMullan, R., Wilson, C., Graham, D., Timms, K. & Warhurst, G. Accuracy of LightCycler® SeptiFast for the detection and identification of pathogens in the blood of patients with suspected sepsis: a systematic review and meta-analysis. *Intensive Care Med.* **41,** 21–33 (2015).

85. Reinhart, K., Bauer, M., Riedemann, N. C. & Hartog, C. S. New approaches to sepsis: molecular diagnostics and biomarkers. *Clin.*

Microbiol. Rev. **25,** 609–34 (2012).

86. Ortiz Ibarra, J., Trevino Valdez, P., Valenzuela Mendez, E., Limon Rojas, A., Lara Flores, G., Ceballos Bocanegra, A., Morales Mendez, I., Fernandez Carrocera, L., Covian Molina, E. & Reyna Figueroa, J. Evaluation of the Light-Cycler® SeptiFast Test in Newborns With Suspicion of Nosocomial Sepsis. *Iran. J. Pediatr.* **25,** e253 (2015).

87. Burdino, E., Ruggiero, T., Allice, T., Milia, M. G., Gregori, G., Milano, R., Cerutti, F., De Rosa, F. G., Manno, E., Caramello, P., Di Perri, G. & Ghisetti, V. Combination of conventional blood cultures and the SeptiFast molecular test in patients with suspected sepsis for the identification of bloodstream pathogens. *Diagn. Microbiol. Infect. Dis.* **79,** 287–292 (2014).

88. Lodes, U., Bohmeier, B., Lippert, H., König, B. & Meyer, F. PCR-based rapid sepsis diagnosis effectively guides clinical treatment in patients with new onset of SIRS. *Langenbeck's Arch. Surg.* **397,** 447–455 (2012).

89. Mancini, N., Carletti, S., Ghidoli, N., Cichero, P., Ossi, C. M., Ieri, R., Poli, E., Burioni, R. & Clementi, M. Molecular diagnosis of polymicrobial sepsis. *J. Clin. Microbiol.* **47,** 1274–5 (2009).

90. Vrioni, G., Daniil, I., Drogari-Apiranthitou, M., Kimouli, M., Papadopoulou, M. & Tsakris, A. Molecular diagnosis of polymicrobial newborn sepsis by multiplex real-time PCR using a small volume of blood sample. *J. Med. Microbiol.* **61,** 1177–1178 (2012).

91. Regueiro, B. J., Varela-Ledo, E., Martinez-Lamas, L., Rodriguez-Calviño, J., Aguilera, A., Santos, A., Gomez-Tato, A. & Alvarez-Escudero, J. Automated Extraction Improves Multiplex Molecular Detection of Infection in Septic Patients. *PLoS One* **5,** e13387 (2010).

92. Tafelski, S., Nachtigall, I., Adam, T., Bereswill, S., Faust, J., Tamarkin, A., Trefzer, T., Deja, M., Idelevich, E. A., Wernecke, K.-D., Becker, K. & Spies, C. Randomized controlled clinical trial evaluating multiplex polymerase chain reaction for pathogen identification and therapy adaptation in critical care patients with pulmonary or abdominal sepsis. *J. Int. Med. Res.* **43,** 364–377 (2015).

93. Fernandez-Cruz, A., Marin, M., Kestler, M., Alcala, L., Rodriguez-Creixems, M. & Bouza, E. The Value of Combining Blood Culture and SeptiFast Data for Predicting Complicated Bloodstream Infections Caused by Gram-Positive Bacteria or Candida Species. *J. Clin.*

Microbiol. **51,** 1130–1136 (2013).

94. Herne, V., Nelovkov, A., Kütt, M. & Ivanova, M. Diagnostic performance and therapeutic impact of LightCycler SeptiFast assay in patients with suspected sepsis. *Eur. J. Microbiol. Immunol. (Bp).* **3,** 68–76 (2013).

95. SepsiTest™-UMD.

96. Horz, H.-P., Scheer, S., Vianna, M. E. & Conrads, G. New methods for selective isolation of bacterial DNA from human clinical specimens. *Anaerobe* **16,** 47–53 (2010).

97. Mühl, H., Kochem, A.-J., Disqué, C. & Sakka, S. G. Activity and DNA contamination of commercial polymerase chain reaction reagents for the universal 16S rDNA real-time polymerase chain reaction detection of bacterial pathogens in blood. *Diagn. Microbiol. Infect. Dis.* **66,** 41–49 (2010).

98. Sakka, S. G., Kochem, A.-J., Disqué, C. & Wellinghausen, N. Blood Infection Diagnosis by 16S rDNA Broad-Spectrum Polymerase Chain Reaction: The Relationship Between Antibiotic Treatment and Bacterial DNA Load. *Anesth. Analg.* **109,** 1707–1708 (2009).

99. Loonen, A. J. M., de Jager, C. P. C., Tosserams, J., Kusters, R., Hilbink, M., Wever, P. C. & van den Brule, A. J. C. Biomarkers and Molecular Analysis to Improve Bloodstream Infection Diagnostics in an Emergency Care Unit. *PLoS One* **9,** e87315 (2014).

100. Kühn, C., Disqué, C., Mühl, H., Orszag, P., Stiesch, M. & Haverich, A. Evaluation of Commercial Universal rRNA Gene PCR plus Sequencing Tests for Identification of Bacteria and Fungi Associated with Infectious Endocarditis. *J. Clin. Microbiol.* **49,** 2919–2923 (2011).

101. Wellinghausen, N., Kochem, A.-J., Disqué, C., Mühl, H., Gebert, S., Winter, J., Matten, J. & Sakka, S. G. Diagnosis of bacteremia in whole-blood samples by use of a commercial universal 16S rRNA gene-based PCR and sequence analysis. *J. Clin. Microbiol.* **47,** 2759–65 (2009).

102. Leitner, E., Kessler, H. H., Spindelboeck, W., Hoenigl, M., Putz-Bankuti, C., Stadlbauer-Köllner, V., Krause, R., Grisold, A. J., Feierl, G. & Stauber, R. E. Comparison of two molecular assays with conventional blood culture for diagnosis of sepsis. *J. Microbiol. Methods* **92,** 253–255 (2013).

103. Nieman, A. E., Savelkoul, P. H. M., Beishuizen, A., Henrich, B., Lamik,

B., MacKenzie, C. R., Kindgen-Milles, D., Helmers, A., Diaz, C., Sakka, S. G. & Schade, R. P. A prospective multicenter evaluation of direct molecular detection of blood stream infection from a clinical perspective. *BMC Infect. Dis.* **16,** 314 (2016).

104. Orszag, P., Disque, C., Keim, S., Lorenz, M. G., Wiesner, O., Hadem, J., Stiesch, M., Haverich, A. & Kuhn, C. Monitoring of Patients Supported by Extracorporeal Membrane Oxygenation for Systemic Infections by Broad-Range rRNA Gene PCR Amplification and Sequence Analysis. *J. Clin. Microbiol.* **52,** 307–311 (2014).

105. Wang, Y., Yang, Q. & Wang, Z. The evolution of nanopore sequencing. *Front. Genet.* **5,** 449 (2015).

106. Oxford Nanopore Technologies 2017.

107. Kilianski, A., Haas, J. L., Corriveau, E. J., Liem, A. T., Willis, K. L., Kadavy, D. R., Rosenzweig, C. & Minot, S. S. Bacterial and viral identification and differentiation by amplicon sequencing on the MinION nanopore sequencer. *Gigascience* **4,** 12 (2015).

108. DNA extraction and library preparation for rapid genus- and species-level identification, with or without PCR.

109. Quick, J., Ashton, P., Calus, S., Chatt, C., Gossain, S., Hawker, J., Nair, S., Neal, K., Nye, K., Peters, T., Pinna, E. De, Robinson, E., Struthers, K., Webber, M., Catto, A., Dallman, T. J., Hawkey, P. & Loman, N. J. Rapid draft sequencing and real-time nanopore sequencing in a hospital outbreak of Salmonella. *Genome Biol.* 1–14 (2015). doi:10.1186/s13059-015-0677-2

110. Schmidt, K., Mwaigwisya, S., Crossman, L. C., Doumith, M., Munroe, D., Pires, C., Khan, A. M., Woodford, N., Saunders, N. J., Wain, J., O'Grady, J. & Livermore, D. M. Identification of bacterial pathogens and antimicrobial resistance directly from clinical urines by nanopore-based metagenomic sequencing. *J. Antimicrob. Chemother.* dkw397 (2016). doi:10.1093/jac/dkw397

111. Benitez-Paez, A., Portune, K. & Sanz, Y. Species-level resolution of 16S rRNA gene amplicons sequenced through MinIONTM portable nanopore sequencer. *Gigascience* **5,** 4 (2015).

112. Mitsuhashi, S., Kryukov, K., Nakagawa, S., Takeuchi, J. S., Shiraishi, Y., Asano, K. & Imanishi, T. A portable system for metagenomic analyses using nanopore-based sequencer and laptop computers can realize

rapid on-site determination of bacterial compositions. *bioRxiv* (2017).

113. Ashton, P. M., Nair, S., Dallman, T., Rubino, S., Rabsch, W., Mwaigwisya, S., Wain, J. & O'Grady, J. MinION nanopore sequencing identifies the position and structure of a bacterial antibiotic resistance island. *Nat Biotech* **33,** 296–300 (2015).

114. Bradley, P., Gordon, N. C., Walker, T. M., Dunn, L., Heys, S., Huang, B., Earle, S., Pankhurst, L. J., Anson, L., de Cesare, M., Piazza, P., Votintseva, A. A., Golubchik, T., Wilson, D. J., Wyllie, D. H., Diel, R., Niemann, S., Feuerriegel, S., Kohl, T. A., Ismail, N., Omar, S. V., Smith, E. G., Buck, D., McVean, G., Walker, A. S., Peto, T., Crook, D., Iqbal, Z. Rapid antibiotic resistance predictions from genome sequence data for S. aureus and M. tuberculosis. *bioRxiv* **6,** 18564 (2015).

115. Fraley, S. I., Hardick, J., Jo Masek, B., Athamanolap, P., Rothman, R. E., Gaydos, C. A., Carroll, K. C., Wakefield, T., Wang, T.-H. H., Yang, S., Masek, B. J., Athamanolap, P., Rothman, R. E., Gaydos, C. A., Carroll, K. C., Wakefield, T., Wang, T.-H. H. & Yang, S. Universal digital high-resolution melt: a novel approach to broad-based profiling of heterogeneous biological samples. *Nucleic Acids Res.*

116. Velez, D. O., Mack, H., Jupe, J., Hawker, S., Kulkarni, N., Hedayatnia, B., Zhang, Y., Lawrence, S. & Fraley, S. I. Massively parallel digital high resolution melt for rapid and absolutely quantitative sequence profiling. *Sci. Rep.* **7,** 42326 (2017).

117. Erali, M., Voelkerding, K. V & Wittwer, C. T. High resolution melting applications for clinical laboratory medicine. *Exp. Mol. Pathol.* **85,** 50–58 (2008).

118. Gundry, C. N., Vandersteen, J. G., Reed, G. H., Pryor, R. J., Chen, J. & Wittwer, C. T. Amplicon melting analysis with labeled primers: a closed-tube method for differentiating homozygotes and heterozygotes. *Clin. Chem.* **49,** 396–406 (2003).

119. Erali, M., Palais, R. & Wittwer, C. SNP genotyping by unlabeled probe melting analysis. *Methods Mol. Biol.* **429,** 199–206 (2008).

120. Dwight, Z., Palais, R. & Wittwer, C. T. uMELT: prediction of high-resolution melting curves and dynamic melting profiles of PCR products in a rich web application. *Bioinformatics* **27,** 1019–1020 (2011).

121. Vernon, S. D., Shukla, S. K., Conradt, J., Unger, E. R. & Reeves, W. C. Analysis of 16S rRNA gene sequences and circulating cell-free DNA

from plasma of chronic fatigue syndrome and non-fatigued subjects. *BMC Microbiol.* **2,** 39 (2002).

122. Ziegler, I., Josefson, P., Olcén, P., Mölling, P. & Strålin, K. Quantitative data from the SeptiFast real-time PCR is associated with disease severity in patients with sepsis. *BMC Infect. Dis.* **14,** 155 (2014).

123. Rogina, P., Skvarc, M., Stubljar, D., Kofol, R. & Kaasch, A. Diagnostic utility of broad range bacterial 16S rRNA gene PCR with degradation of human and free bacterial DNA in bloodstream infection is more sensitive than an in-house developed PCR without degradation of human and free bacterial DNA. *Mediators Inflamm.* **2014,** 108592 (2014).

124. Schreiber, J., Nierhaus, A., Braune, S. A., de Heer, G. & Kluge, S. Comparison of three different commercial PCR assays for the detection of pathogens in critically ill sepsis patients. *Medizinische Klin. - Intensivmed. und Notfallmedizin* **108,** 311–318 (2013).

125. Caliendo, A. M., Gilbert, D. N., Ginocchio, C. C., Hanson, K. E., May, L., Quinn, T. C., Tenover, F. C., Alland, D., Blaschke, A. J., Bonomo, R. A., Carroll, K. C., Ferraro, M. J., Hirschhorn, L. R., Joseph, W. P., Karchmer, T., MacIntyre, A. T., Reller, L. B. & Jackson, A. F. Better Tests, Better Care: Improved Diagnostics for Infectious Diseases. *Clin. Infect. Dis.* **57,** S139–S170 (2013).

126. Wilson, I. G. Inhibition and facilitation of nucleic acid amplification. *Appl. Environ. Microbiol.* **63,** 3741–51 (1997).

127. Rantakokko-Jalava, K. & Jalava, J. Optimal DNA Isolation Method for Detection of Bacteria in Clinical Specimens by Broad-Range PCR. *J. Clin. Microbiol.* **40,** 4211–4217 (2002).

128. Morata, P., Queipo-Ortuño, M. I. & de Dios Colmenero, J. Strategy for optimizing DNA amplification in a peripheral blood PCR assay used for diagnosis of human brucellosis. *J. Clin. Microbiol.* **36,** 2443–6 (1998).

129. Immunexpress Inc.

130. Mchugh, L., Seldon, T. A., Brandon, R. A., Kirk, J. T., Rapisarda, A., Sutherland, A. J., Presneill, J. J., Venter, D. J., Lipman, J., Thomas, M. R., Klouwenberg, P. M. C. K. & Van, L. RESEARCH ARTICLE A Molecular Host Response Assay to Discriminate Between Sepsis and Infection- Negative Systemic Inflammation in Critically Ill Patients : Discovery and Validation in Independent Cohorts. 1–35 (2015). doi:10.1371/journal.pmed.1001916

131. Zimmerman, J. J., Sullivan, E., Yager, T. D., Cheng, C., Permut, L., Cermelli, S., Mchugh, L., Sampson, D., Seldon, T., Brandon, R. B. & Brandon, R. A. Diagnostic Accuracy of a Host Gene Expression Signature That Discriminates Clinical Severe Sepsis Syndrome and Infection-Negative Systemic Inflammation Among Critically Ill Children. **45,** (2017).

132. Zimmerman, J., Sullivan, E., Sampson, D., McHugh, L., Yager, T. & Seldon, T. SENSITIVE AND SPECIFIC DIAGNOSIS OF SEPSIS IN CRITICALLY ILL CHILDREN UTILIZING HOST GENE EXPRESSION. *Crit. Care Med.* **43,** 258 (2015).

133. Miller, R., Lopansri, B., McHugh, L., Rapisarda, A., Seldon, T. & Burke, J. VALIDATION OF A NOVEL HOST RESPONSE ASSAY TO DISTINGUISH SIRS AND SEPSIS IN CRITICALLY ILL PATIENTS. *Crit. Care Med.* **43,** 252 (2015).

134. Law, J. W.-F., Ab Mutalib, N.-S., Chan, K.-G. & Lee, L.-H. Rapid methods for the detection of foodborne bacterial pathogens: principles, applications, advantages and limitations. *Front. Microbiol.* **5,** 770 (2014).

135. Zhao, X., Lin, C.-W., Wang, J. & Oh, D. H. Advances in rapid detection methods for foodborne pathogens. *J. Microbiol. Biotechnol.* **24,** 297–312 (2014).

136. Connelly, J. T., Rolland, J. P. & Whitesides, G. M. "Paper Machine" for Molecular Diagnostics. *Anal. Chem.* **87,** 7595–7601 (2015).

137. Safavieh, M., Kanakasabapathy, M. K., Tarlan, F., Ahmed, M. U., Zourob, M., Asghar, W. & Shafiee, H. Emerging Loop-Mediated Isothermal Amplification-Based Microchip and Microdevice Technologies for Nucleic Acid Detection. *ACS Biomater. Sci. Eng.* **2,** 278–294 (2016).

138. Buchan, B. W. & Ledeboer, N. A. Emerging technologies for the clinical microbiology laboratory. *Clin. Microbiol. Rev.* **27,** 783–822 (2014).

139. Misawa, Y., Saito, R., Moriya, K., Koike, K., Yoshida, A., Okuzumi, K., Yoshida, H., Misawa, Y., Ito, N. & Okada, M. Application of loop-mediated isothermal amplification technique to rapid and direct detection of methicillin-resistant Staphylococcus aureus (MRSA) in blood cultures. *J. Infect. Chemother.* **13,** 134–140 (2007).

140. Macarthur, G. Global health diagnostics : research , development and regulation Workshop report. (2009).

141. Kang, D.-K., Ali, M. M., Zhang, K., Huang, S. S., Peterson, E., Digman, M. a, Gratton, E. & Zhao, W. Rapid detection of single bacteria in unprocessed blood using Integrated Comprehensive Droplet Digital Detection. *Nat. Commun.* **5,** 5427 (2014).

142. Skinner, J. P., Swift, K. M., Ruan, Q., Perfetto, S., Gratton, E. & Tetin, S. Y. Simplified confocal microscope for counting particles at low concentrations. *Rev. Sci. Instrum.* **84,** 74301 (2013).

143. Altamore, I., Lanzano, L. & Gratton, E. Dual channel detection of ultra low concentration of bacteria in real time by scanning FCS. *Meas. Sci. Technol.* **24,** 65702 (2013).

144. UC Irvine News: November 13, 2014.

145. Medical Predictive Science Corporation (MPSC).

146. Moorman, J. R., Carlo, W. A., Kattwinkel, J., Schelonka, R. L., Porcelli, P. J., Navarrete, C. T., Bancalari, E., Aschner, J. L., Walker, M. W., Perez, J. A., Palmer, C., Stukenborg, G. J., Lake, D. E. & O'Shea, T. M. Mortality reduction by heart rate characteristic monitoring in very low birth weight neonates: a randomized trial. *J. Pediatr.* **159,** 900–906.e1 (2011).

147. Sullivan, B. A., Grice, S. M., Lake, D. E., Moorman, J. R. & Fairchild, K. D. INFECTION AND OTHER CLINICAL CORRELATES OF ABNORMAL HEART RATE CHARACTERISTICS IN PRETERM INFANTS. *J. Pediatr.* **164,** 775–780 (2014).

148. Coggins, S. A., Weitkamp, J.-H., Grunwald, L., Stark, A. R., Reese, J., Walsh, W. & Wynn, J. L. Heart rate characteristic index monitoring for bloodstream infection in an NICU: a 3-year experience. *Arch. Dis. Child. Fetal Neonatal Ed.* **101,** F329-32 (2016).

149. Wang, K., Bhandari, V., Chepustanova, S., Huber, G., O'Hara, S., O'Hern, C. S., Shattuck, M. D. & Kirby, M. Which biomarkers reveal neonatal sepsis? *PLoS One* **8,** e82700 (2013).

150. Mani, S., Ozdas, A., Aliferis, C., Varol, H. A., Chen, Q., Carnevale, R., Chen, Y., Romano-Keeler, J., Nian, H. & Weitkamp, J.-H. Medical decision support using machine learning for early detection of late-onset neonatal sepsis. *J. Am. Med. Inform. Assoc.* **21,** 326–336 (2014).

151. Henry, K. E., Hager, D. N., Pronovost, P. J. & Saria, S. A targeted real-time early warning score (TREWScore) for septic shock. *Sci. Transl.*

Med. **7,** 299ra122 (2015).

152. Song, L., Shan, D., Zhao, M., Pink, B. A., Minnehan, K. A., York, L., Gardel, M., Sullivan, S., Phillips, A. F., Hayman, R. B., Walt, D. R. & Duffy, D. C. Direct Detection of Bacterial Genomic DNA at Sub-Femtomolar Concentrations Using Single Molecule Arrays. *Anal. Chem.* **85,** 1932–1939 (2013).

153. Patel, R. MALDI-TOF MS for the Diagnosis of Infectious Diseases. *Clin. Chem.* **61,** 100–111 (2015).

154. Frey, K. G., Herrera-Galeano, J. E., Redden, C. L., Luu, T. V, Servetas, S. L., Mateczun, A. J., Mokashi, V. P. & Bishop-Lilly, K. A. Comparison of three next-generation sequencing platforms for metagenomic sequencing and identification of pathogens in blood. *BMC Genomics* **15,** 96 (2014).

155. Lisboa, T., Waterer, G. & Rello, J. We should be measuring genomic bacterial load and virulence factors: *Crit. Care Med.* **38,** S656–S662 (2010).

156. Pasic, M. D., Samaan, S. & Yousef, G. M. Genomic Medicine: New Frontiers and New Challenges. *Clin. Chem.* **59,** 158–167 (2013).

157. Pritchard, C. C., Cheng, H. H. & Tewari, M. MicroRNA profiling: approaches and considerations. *Nat. Rev. Genet.* **13,** 358–369 (2012).

158. Blainey, P. C. The future is now: single-cell genomics of bacteria and archaea. *FEMS Microbiol. Rev.* **37,** 407–427 (2013).

159. Reed, G. H. & Wittwer, C. T. Sensitivity and Specificity of Single-Nucleotide Polymorphism Scanning by High-Resolution Melting Analysis. *Clin. Chem.* **50,** 1748–1754 (2004).

160. Chakravorty, S., Lee, J. S., Cho, E. J., Roh, S. S., Smith, L. E., Lee, J., Kim, C. T., Via, L. E., Cho, S.-N., Barry, C. E. & Alland, D. Genotypic Susceptibility Testing of Mycobacterium tuberculosis Isolates for Amikacin and Kanamycin Resistance by Use of a Rapid Sloppy Molecular Beacon-Based Assay Identifies More Cases of Low-Level Drug Resistance than Phenotypic Lowenstein-Jensen Testin. *J. Clin. Microbiol.* **53,** 43–51 (2015).

161. El-Hajj, H. H., Marras, S. A. E., Tyagi, S., Shashkina, E., Kamboj, M., Kiehn, T. E., Glickman, M. S., Kramer, F. R. & Alland, D. Use of Sloppy Molecular Beacon Probes for Identification of Mycobacterial Species. *J.*

Clin. Microbiol. **47,** 1190–1198 (2009).

162. Vossen, R. H. A. M., Aten, E., Roos, A. & den Dunnen, J. T. High-Resolution Melting Analysis (HRMA)—More than just sequence variant screening. *Hum. Mutat.* **30,** 860–866 (2009).

163. Mohamed Suhaimi, N.-A., Foong, Y. M., Lee, D. Y. S., Phyo, W. M., Cima, I., Lee, E. X. W., Goh, W. L., Lim, W.-Y., Chia, K. S., Kong, S. L., Gong, M., Lim, B., Hillmer, A. M., Koh, P. K., Ying, J. Y. & Tan, M.-H. Non-invasive sensitive detection of KRAS and BRAF mutation in circulating tumor cells of colorectal cancer patients. *Mol. Oncol.* **9,** 850–860 (2015).

164. Athamanolap, P., Shin, D. J. & Wang, T.-H. Droplet Array Platform for High-Resolution Melt Analysis of DNA Methylation Density. *J. Lab. Autom.* **19,** 304–312 (2014).

165. Lorente, A., Mueller, W., Urdangarín, E., Lázcoz, P., von Deimling, A. & Castresana, J. S. Detection of methylation in promoter sequences by melting curve analysis-based semiquantitative real time PCR. *BMC Cancer* **8,** 61 (2008).

166. Gurtler, V, Grando, D., Mayall, B. C., Wang, J. & Ghaly-Derias, S. A novel method for simultaneous Enterococcus species identification/typing and van genotyping by high resolution melt analysis. *J. Microbiol. Methods* **90,** 167–181 (2012).

167. Hjelmsø, M. H., Hansen, L. H., Bælum, J., Feld, L., Holben, W. E. & Jacobsen, C. S. High-Resolution Melt Analysis for Rapid Comparison of Bacterial Community Compositions. *Appl. Environ. Microbiol.* **80,** 3568–3575 (2014).

168. Hardick, J., Won, H., Jeng, K., Hsieh, Y.-H., Gaydos, C. A., Rothman, R. E. & Yang, S. Identification of Bacterial Pathogens in Ascitic Fluids from Patients with Suspected Spontaneous Bacterial Peritonitis by Use of Broad-Range PCR (16S PCR) Coupled with High-Resolution Melt Analysis. *J. Clin. Microbiol.* **50,** 2428–2432 (2012).

169. Jeng, K., Yang, S., Won, H., Gaydos, C. A., Hsieh, Y.-H., Kecojevic, A., Carroll, K. C., Hardick, J. & Rothman, R. E. Application of a 16S rRNA PCR–High-Resolution Melt Analysis Assay for Rapid Detection of Salmonella Bacteremia. *J. Clin. Microbiol.* **50,** 1122–1124 (2012).

170. Masek, B. J., Hardick, J., Won, H., Yang, S., Hsieh, Y.-H., Rothman, R. E. & Gaydos, C. A. Sensitive Detection and Serovar Differentiation of

Typhoidal and Nontyphoidal Salmonella enterica Species Using 16S rRNA Gene PCR Coupled with High-Resolution Melt Analysis. *J. Mol. Diagnostics* **16,** 261–266 (2014).

171. Yang, S., Ramachandran, P., Rothman, R., Hsieh, Y.-H., Hardick, A., Won, H., Kecojevic, A., Jackman, J. & Gaydos, C. Rapid Identification of Biothreat and Other Clinically Relevant Bacterial Species by Use of Universal PCR Coupled with High-Resolution Melting Analysis. *J. Clin. Microbiol.* **47,** 2252–2255 (2009).

172. Fraley, S. I., Hardick, J., Jo Masek, B., Athamanolap, P., Rothman, R. E., Gaydos, C. A., Carroll, K. C., Wakefield, T., Wang, T.-H. & Yang, S. Universal digital high-resolution melt: a novel approach to broad-based profiling of heterogeneous biological samples. *Nucleic Acids Res.* **41,** e175–e175 (2013).

173. Fraley, S. I., Athamanolap, P., Masek, B. J., Hardick, J., Carroll, K. C., Hsieh, Y.-H., Rothman, R. E., Gaydos, C. A., Wang, T.-H. & Yang, S. Nested Machine Learning Facilitates Increased Sequence Content for Large-Scale Automated High Resolution Melt Genotyping. *Sci. Rep.* **6,** 19218 (2016).

174. Fan, J.-B., Chee, M. S. & Gunderson, K. L. Highly parallel genomic assays. *Nat. Rev. Genet.* **7,** 632–644 (2006).

175. Athamanolap, P., Parekh, V., Fraley, S. I., Agarwal, V., Shin, D. J., Jacobs, M. A., Wang, T.-H. & Yang, S. Trainable High Resolution Melt Curve Machine Learning Classifier for Large-Scale Reliable Genotyping of Sequence Variants. *PLoS One* **9,** e109094 (2014).

176. Candiloro, I. L. M., Mikeska, T., Hokland, P. & Dobrovic, A. Rapid analysis of heterogeneously methylated DNA using digital methylation-sensitive high resolution melting: application to the CDKN2B (p15) gene. *Epigenetics Chromatin* **1,** 7 (2008).

177. Zou, H., Taylor, W. R., Harrington, J. J., Hussain, F. T. N., Cao, X., Loprinzi, C. L., Levine, T. R., Rex, D. K., Ahnen, D., Knigge, K. L., Lance, P., Jiang, X., Smith, D. I. & Ahlquist, D. A. High Detection Rates of Colorectal Neoplasia by Stool DNA Testing With a Novel Digital Melt Curve Assay. *Gastroenterology* **136,** 459–470 (2009).

178. Pritt, B. S., Mead, P. S., Johnson, D. K. H., Neitzel, D. F., Respicio-Kingry, L. B., Davis, J. P., Schiffman, E., Sloan, L. M., Schriefer, M. E., Replogle, A. J., Paskewitz, S. M., Ray, J. A., Bjork, J., Steward, C. R., Deedon, A., Lee, X., Kingry, L. C., Miller, T. K., Feist, M. A., Theel, E. S.,

Patel, R., Irish, C. L., Petersen, J. M. Identification of a novel pathogenic Borrelia species causing Lyme borreliosis with unusually high spirochaetaemia: a descriptive study. *Lancet Infect. Dis.* **16,** 556–564 (2016).

179. Dietzman, D. E., Fischer, G. W. & Schoenknecht, F. D. Neonatal escherichia coli septicemia—bacterial counts in blood. *J. Pediatr.* **85,** 128–130 (1974).

180. Kellogg, J. A., Manzella, J. P. & Bankert, D. A. Frequency of low-level bacteremia in children from birth to fifteen years of age. *J. Clin. Microbiol.* **38,** 2181–5 (2000).

181. Chakravorty, S., Helb, D., Burday, M., Connell, N. & Alland, D. A detailed analysis of 16S ribosomal RNA gene segments for the diagnosis of pathogenic bacteria. *J. Microbiol. Methods* **69,** 330–339 (2007).

182. Simonsen, K. A., Anderson-Berry, A. L., Delair, S. F. & Davies, H. D. Early-Onset Neonatal Sepsis. *Clin. Microbiol. Rev.* **27,** 21–47 (2014).

183. Mohammadi, T., Reesink, H. W., Vandenbroucke-Grauls, C. M. J. E. & Savelkoul, P. H. M. Optimization of Real-Time PCR Assay for Rapid and Sensitive Detection of Eubacterial 16S Ribosomal DNA in Platelet Concentrates. *J. Clin. Microbiol.* **41,** 4796–4798 (2003).

184. Rothman, R. E., Majmudar, M. D., Kelen, G. D., Madico, G., Gaydos, C. A., Walker, T. & Quinn, T. C. Detection of Bacteremia in Emergency Department Patients at Risk for Infective Endocarditis Using Universal 16S rRNA Primers in a Decontaminated Polymerase Chain Reaction Assay. *J. Infect. Dis.* **186,** 1677–1681 (2002).

185. Salter, S. J., Cox, M. J., Turek, E. M., Calus, S. T., Cookson, W. O., Moffatt, M. F., Turner, P., Parkhill, J., Loman, N. J. & Walker, A. W. Reagent and laboratory contamination can critically impact sequence-based microbiome analyses. *BMC Biol.* **12,** 87 (2014).

186. Spangler, R., Goddard, N. L. & Thaler, D. S. Optimizing Taq Polymerase Concentration for Improved Signal-to-Noise in the Broad Range Detection of Low Abundance Bacteria. *PLoS One* **4,** e7010 (2009).

187. Mallona, I., Weiss, J. & Egea-Cortines, M. pcrEfficiency: a Web tool for PCR amplification efficiency prediction. *BMC Bioinformatics* **12,** 404 (2011).

188. Rothfuss, O., Gasser, T. & Patenge, N. Analysis of differential DNA damage in the mitochondrial genome employing a semi-long run real-time PCR approach. *Nucleic Acids Res.* **38,** e24 (2010).

189. McGowan, K. L., Foster, J. A. & Coffin, S. E. Outpatient pediatric blood cultures: time to positivity. *Pediatrics* **106,** 251–255 (2000).

190. Nixon, G., Garson, J. A., Grant, P., Nastouli, E., Foy, C. A. & Huggett, J. F. Comparative Study of Sensitivity, Linearity, and Resistance to Inhibition of Digital and Nondigital Polymerase Chain Reaction and Loop Mediated Isothermal Amplification Assays for Quantification of Human Cytomegalovirus. *Anal. Chem.* **86,** 4387–4394 (2014).